

Supplementary Materials

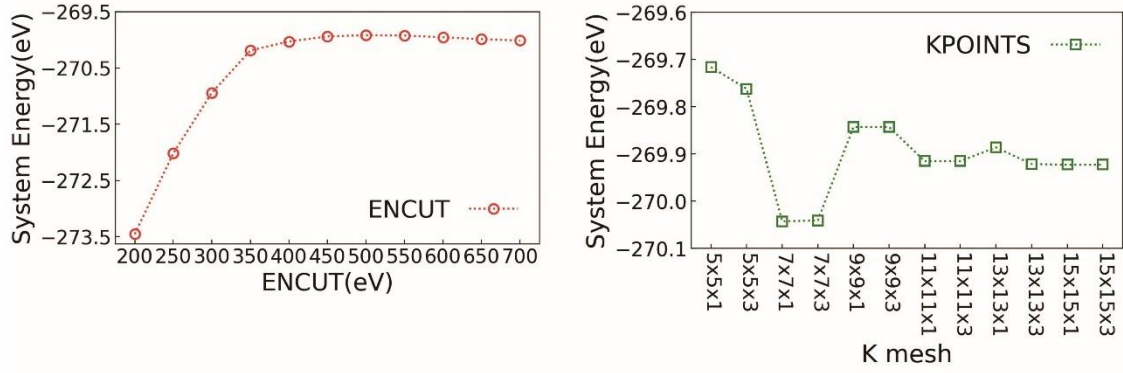
Theoretical investigation on the self-organized MXene heterostructures: interface, sliding and Li/Na ion storage application

Dundong Yuan¹, Yuwei Xiong¹, Litao Sun¹, Weiwei Sun², Chao Zhu¹

¹SEU-FEI Nano-Pico Center, Key Laboratory of MEMS of Ministry of Education, School of Integrated Circuits, Southeast University, Nanjing 210096, Jiangsu, China.

²Key Laboratory of Quantum Materials and Devices of Ministry of Education, School of Physics, Southeast University, Nanjing 211189, Jiangsu, China.

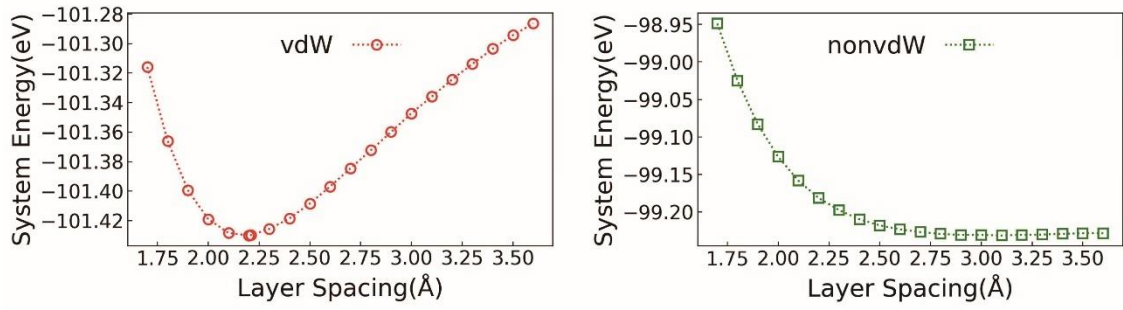
Correspondence to: Prof. Chao Zhu, SEU-FEI Nano-Pico Center, Key Lab of MEMS of Ministry of Education, School of Integrated Circuits, Southeast University, Nanjing 210096, Jiangsu, China. E-mail: zhuchao@seu.edu.cn; Prof. Weiwei Sun, Key Laboratory of Quantum Materials and Devices of Ministry of Education, School of Physics, Southeast University, Nanjing 211189, Jiangsu, China. E-mail: Sun_weiwei@seu.edu.cn



Supplementary Figure 1. The convergence test of ENCUT and KPOINTS using 3Ti1Nb bulk models.

MXene	a(Å)	t(Å)	d(Å)	Δ Bader(M)	Δ Bader(T)	WF
Nb ₂ CF ₂	3.10229	7.35	2.20167	-1.59	0.73	4.48 ^[1]
Nb ₂ CO ₂	3.09459	7.11	2.37424	-1.95	1.08	5.81 ^[1]
Nb ₂ C(OH) ₂	3.12619	7.62	0.44966	-1.57	0.71	2.15 ^[1]
Ti ₃ C ₂ F ₂	3.06069	9.40	2.223415	-1.69	0.75	4.98 ^[1]
Ti ₃ C ₂ O ₂	3.02422	9.38	2.444355	-1.84	1.10	6.16 ^[1]
Ti ₃ C ₂ (OH) ₂	3.07641	9.75	0.522175	-1.67	0.72	1.81 ^[1]
Ti ₃ C ₂ O ₂ ^[2]	3.057					5.94
Ti ₃ C ₂ (OH) ₂	3.105					1.57
[2]						
Nb ₂ C ^[3]	3.135					

Supplementary Table 1. Parameters of pure MXenes calculated in this work in comparison with previous reported data. a: Lattice length of a(b) axis; t: layer thickness; d: layer spacings (distance between the upmost and downmost atoms at the interspace along c-axis direction); Δ Bader(M): Bader change of surficial metal atoms; Δ Bader(T): Bader change of functional groups; WF: work functions.

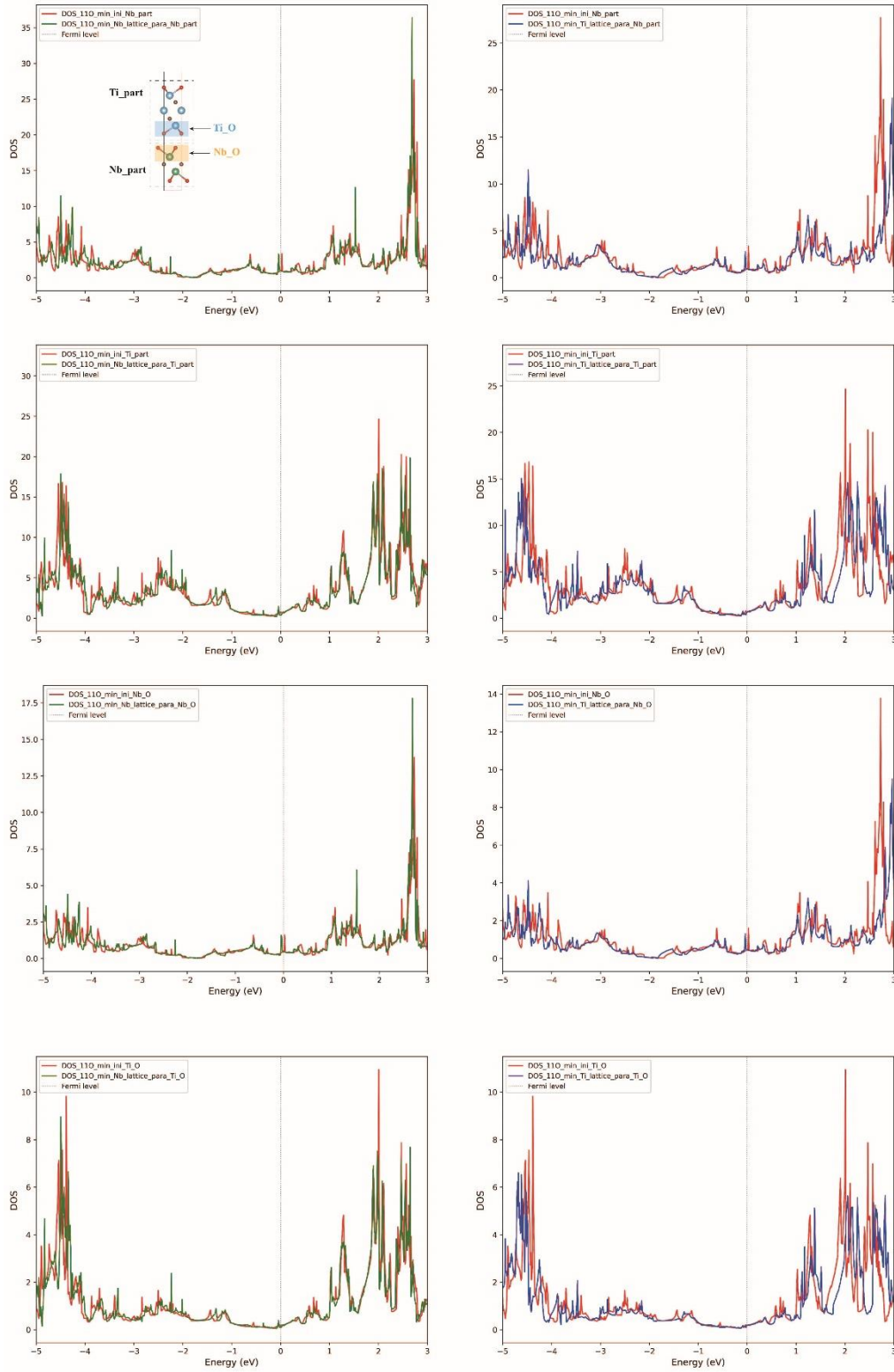


Supplementary Figure 2. The convergence test comparing self-consistent field calculation with and without van der Waals interaction (IVDW = 11).

Models	E_Nb_avg	E_Nb_native	E_Ti_avg	E_Ti_native	$\Delta E_{\text{strain_total}}$
A0Z0	-47.7792	-47.8165	-64.6441	-64.7209	0.1141
A0Z1	-47.7818	-47.8164	-64.6414	-64.7208	0.1140
A0Z2	-47.7759	-47.8164	-64.6471	-64.7207	0.1141
A0Z4	-47.7744	-47.8164	-64.6488	-64.7207	0.1139
A0Z5	-47.7797	-47.8165	-64.6436	-64.7207	0.1139
Z0A1	-47.7801	-47.8164	-64.6430	-64.7208	0.1141
Z0A2	-47.7749	-47.8164	-64.6484	-64.7209	0.1140
Z0A3	-47.7752	-47.8164	-64.6480	-64.7208	0.1140
Z0A4	-47.7702	-47.8164	-64.6527	-64.7208	0.1143
Z0A5	-47.7818	-47.8164	-64.6414	-64.7208	0.1141
Z1A1	-47.7762	-47.8164	-64.6468	-64.7207	0.1141
Z1A2	-47.7764	-47.8164	-64.6470	-64.7208	0.1139
Z1A4	-47.7756	-47.8164	-64.6474	-64.7207	0.1141
Z1A5	-47.7750	-47.8165	-64.6481	-64.7207	0.1141
Z2A1	-47.7755	-47.8164	-64.6476	-64.7207	0.1140
Z2A2	-47.7760	-47.8164	-64.6471	-64.7207	0.1140
Z2A4	-47.7754	-47.8164	-64.6477	-64.7207	0.1140
Z2A5	-47.7761	-47.8164	-64.6472	-64.7208	0.1139

Supplementary Table 2. The calculated strain energies for all 1Ti1Nb -O sliding models. The upper limit of strain energy for the heterostructure was then evaluated as $\Delta E_{\text{strain_total}} = (E_{\text{Ti_avg}} - E_{\text{Ti_native}}) + (E_{\text{Nb_avg}} - E_{\text{Nb_native}})$. Where

$AxZy$ stands for $AM_x*\delta/6ZZ_y*\delta/6$, and $BxAy$ is similar. The unit of data here is eV.

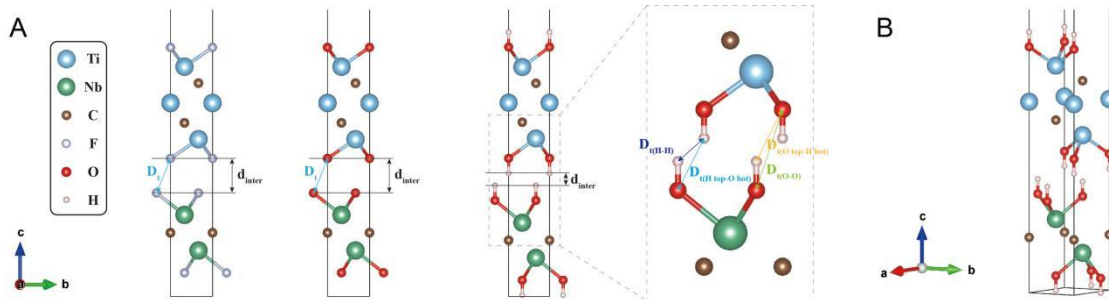


Supplementary Figure 3. The impacts of lattice mismatch on PDOS of 1Ti1Nb -O ground state model (110_min). “ini” means average lattice parameter,

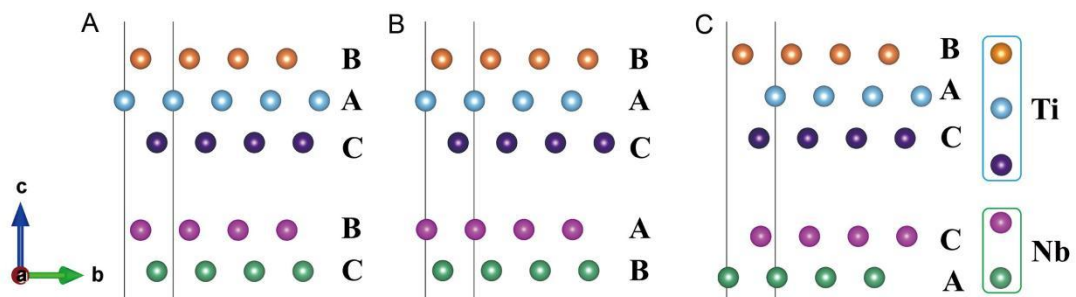
“Ti_lattice_para”, “Nb_lattice_para” means lattice parameter of native $\text{Ti}_3\text{C}_2\text{O}_2$ and Nb_2CO_2 models.

	Z0	Z1	Z2	Z3	Z4	Z5	Z6
A0	0, 0	-1/6, -1/6	-1/3, -1/3	-1/2, -1/2	-2/3, -2/3	-5/6, -5/6	-1, -1
A1	1/6, -1/6	0, -1/3	-1/6, -1/2	-1/3, -2/3	-1/2, -5/6	-2/3, -1	-5/6, -7/6
A2	1/3, -1/3	1/6, -1/2	0, -2/3	-1/6, -5/6	-1/3, -1	-1/2, -7/6	-2/3, -4/3
A3	1/2, -1/2	1/3, -2/3	1/6, -5/6	0, -1	-1/6, -7/6	-1/3, -4/3	-1/2, -3/2
A4	2/3, -2/3	1/2, -5/6	1/3, -1	1/6, -7/6	0, -4/3	-1/6, -3/2	-1/3, -5/3
A5	5/6, -5/6	2/3, -1	1/2, -7/6	1/3, -4/3	1/6, -3/2	0, -5/3	-1/6, -11/6
A6	1, -1	5/6, -7/6	2/3, -4/3	1/2, -3/2	1/3, -5/3	1/6, -11/6	0, -2

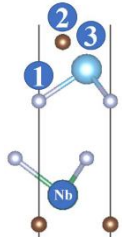
Supplementary Table 3. The relative location of Nb_2CT_x in sliding comparing with the original location. (x, y) numbers in the chart are abbreviations of $(x \cdot V_{AM}, y \cdot V_{ZZ})$, in which V_{AM} and V_{ZZ} refers to the minimal vectors along AM and ZZ.



Supplementary Figure 4. The definition of d_{inter} and D_t . (A) shows how d_{inter} and D_t are measured, taking 1Ti1Nb A0Z0 models as examples; (B) shows the -OH terminated model viewing from the standard orientation of crystal shape in VESTA.



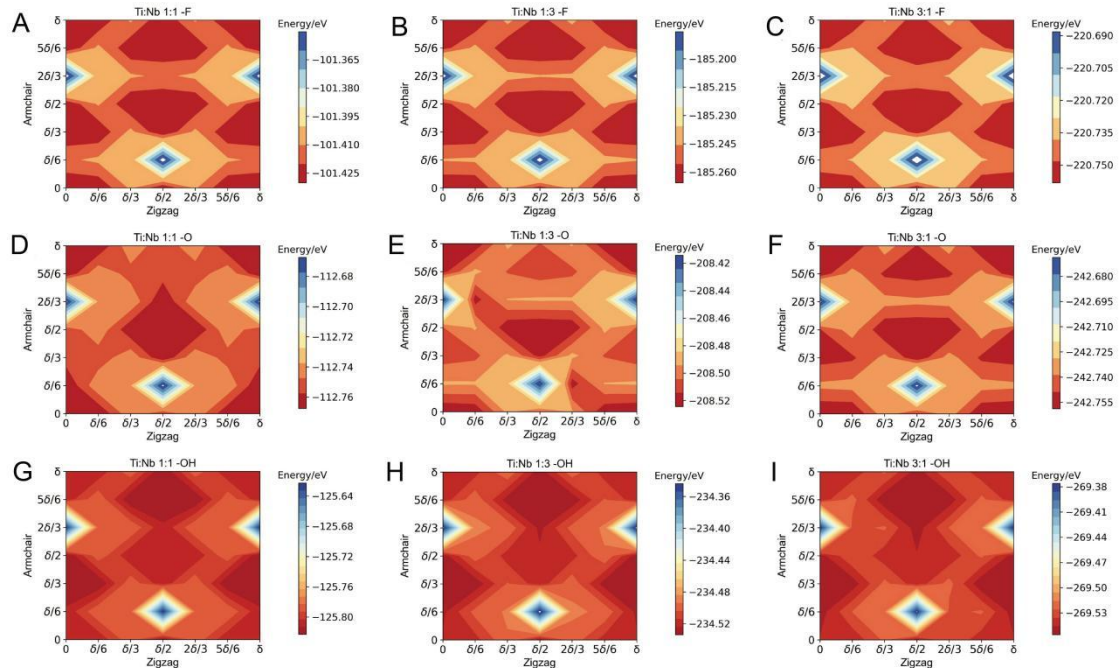
Supplementary Figure 5. Metal atoms stacking of models with minimum and maximum energies. (A) Ground-state model AM_0ZZ_0 with FCC stacking metal atoms (BAC-BC) corresponding to; (B) Ground-state model $AM_{\delta/3}ZZ_0$ with FCC stacking metal atoms (BAC-AB); (C) Maximum-energy model $AM_{2\delta/3}ZZ_0$ with a twin grain boundary (BAC-CA). Different layers of Ti atoms are displayed by orange, blue and purple balls, and different layers of Nb atoms are displayed by pink and green balls.



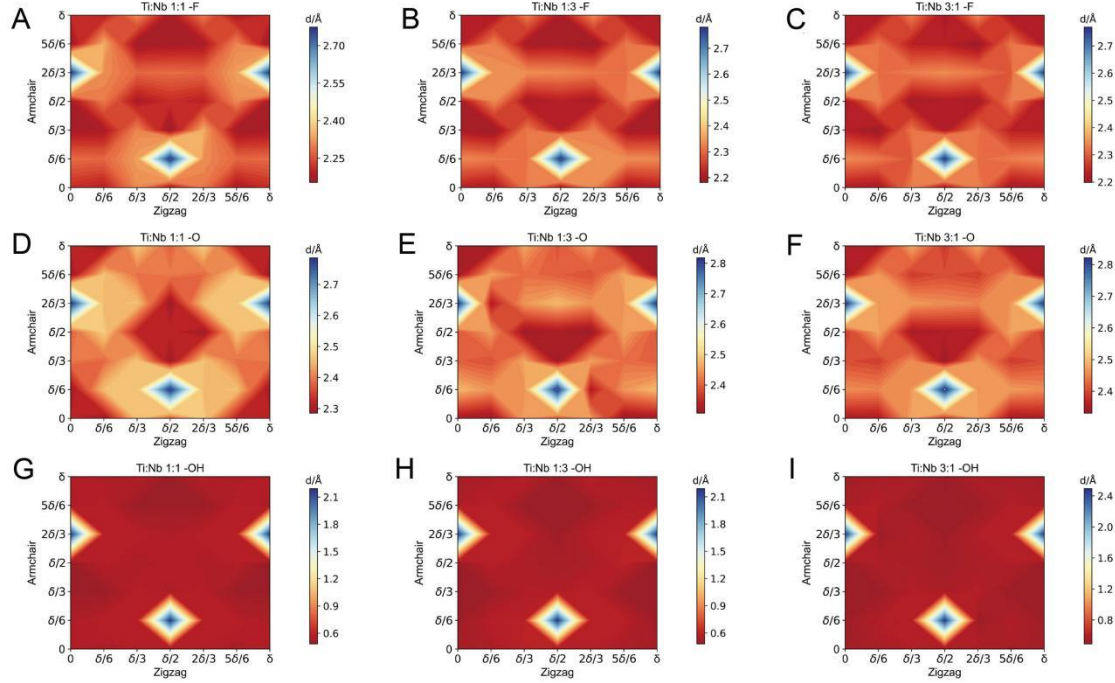
1:1 F 1:1 O 1:1 OH 1:3 F 1:3 O 1:3 OH 3:1 F 3:1 O 3:1 OH

Nb atom 2 2 1 2 2 1 1 2 1

Supplementary Table 4. The relative locations of Nb atoms at interspace with different layer ratios and terminations. Numbers 1, 2 and 3 represents locations of terminations, C atoms and Ti atoms. After relaxation, Nb atoms of most stable models align with one of these three locations.



Supplementary Figure 6. Full-period energy variation for sliding of each type of heterostructure, layer-ratios are 1:1, 1:3 and 3:1 from left to right, and functional groups are -F, -O, -OH, from top to bottom respectively.



Supplementary Figure 7. Full-period layer distance variation for sliding of each type of heterostructure, layer-ratios are 1:1, 1:3 and 3:1 from left to right, and functional groups are -F, -O, -OH, from top to bottom respectively.

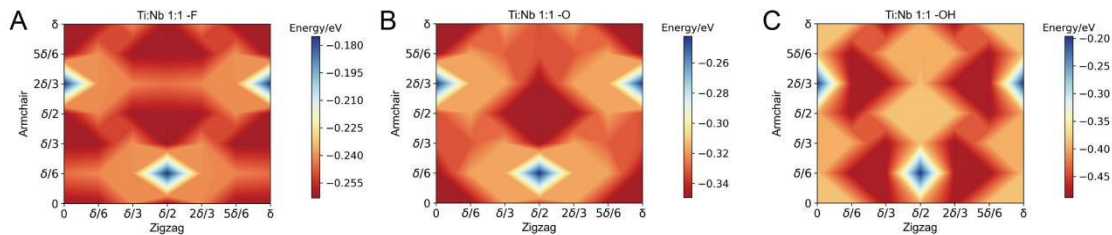
	ΔE (Ti) /meV	range	ΔE (Nb) /meV	range	ΔE (Binding) /meV	range
1:1 -F	8.54		6.27		1928.90	
1:1 -O	16.03		11.65		1273.20	
1:1 -OH	91.47		62.70		3050.4	

Supplementary Table 5. Energy variation ranges of $Ti_3C_2T_x$ parts, Nb_2CT_x parts and binding energies for 1Ti1Nb with different terminations.

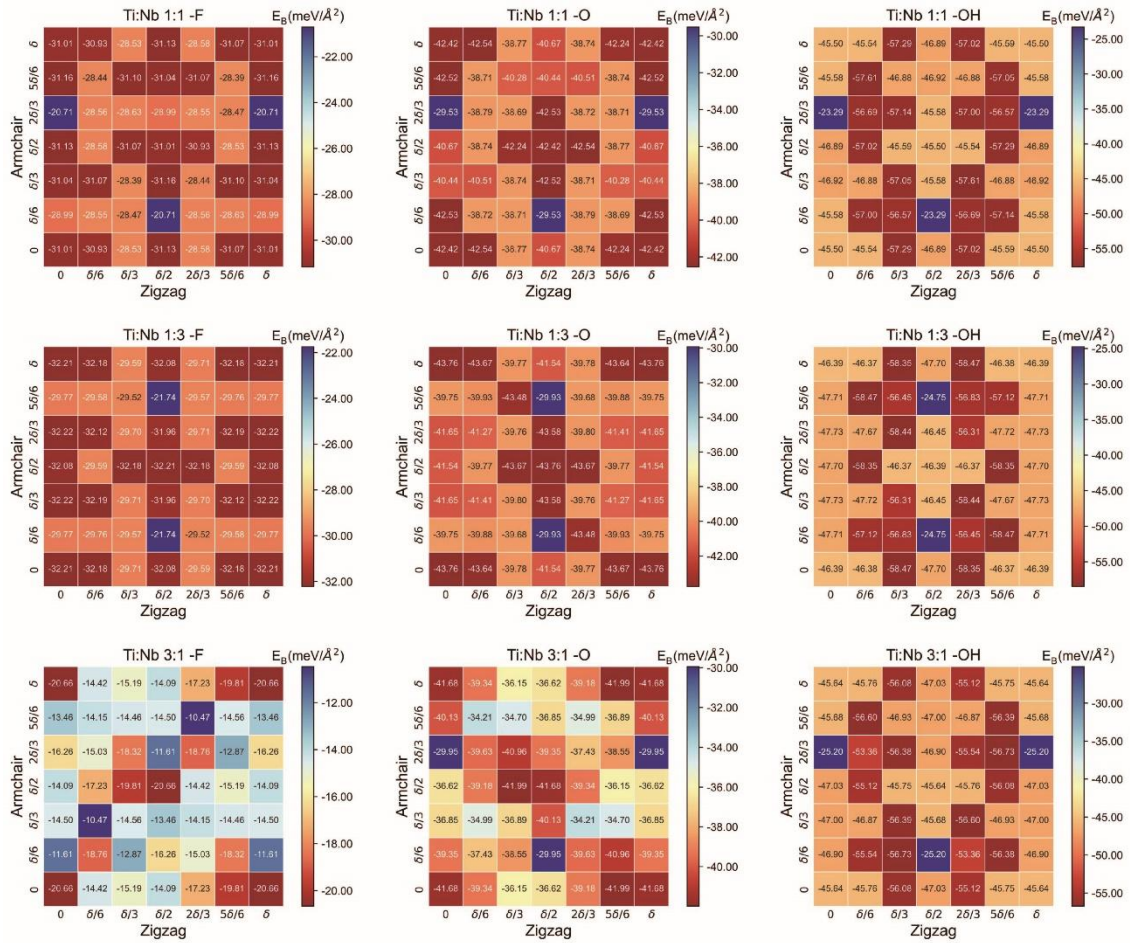
Z0	Z1	Z2	Z3	Z4	Z5	Z6
----	----	----	----	----	----	----

A0	-0.2618	-0.2612	-0.2409	-0.2630	-0.2413	-0.2625	-0.2618
A1	-0.2447	-0.2411	-0.2403	-0.1746	-0.2410	-0.2418	-0.2447
A2	-0.2622	-0.2625	-0.2397	-0.2633	-0.2399	-0.2628	-0.2622
A3	-0.2630	-0.2413	-0.2625	-0.2618	-0.2612	-0.2409	-0.2630
A4	-0.1746	-0.2410	-0.2418	-0.2447	-0.2411	-0.2403	-0.1746
A5	-0.2633	-0.2399	-0.2628	-0.2622	-0.2625	-0.2397	-0.2633
A6	-0.2618	-0.2612	-0.2409	-0.2630	-0.2413	-0.2625	-0.2618

Supplementary Table 6. The calculated binding energies for all 1Ti1Nb -F sliding models. The binding energy of the 1Ti1Nb -F (1 layer of $Ti_3C_2F_2$ + 1 layer of Nb_2CF_2) heterostructure was calculated as $E_B = E_{MX_{ene}} - (E_{Ti_3C_2F_2} + E_{Nb_2CF_2})$. Where $AxZy$ stands for $AM_x*\delta/6ZZ_y*\delta/6$, and $BxAy$ is similar. The unit of data here is eV. Data of other models are accessible in supplementary excel “Energy vs. dinter (Dt)_Energy_sigma_0”.



Supplementary Figure 8. The full-period binding energy variation for sliding of 1Ti1Nb heterostructure, functional groups are -F, -O, -OH, from left to right respectively.

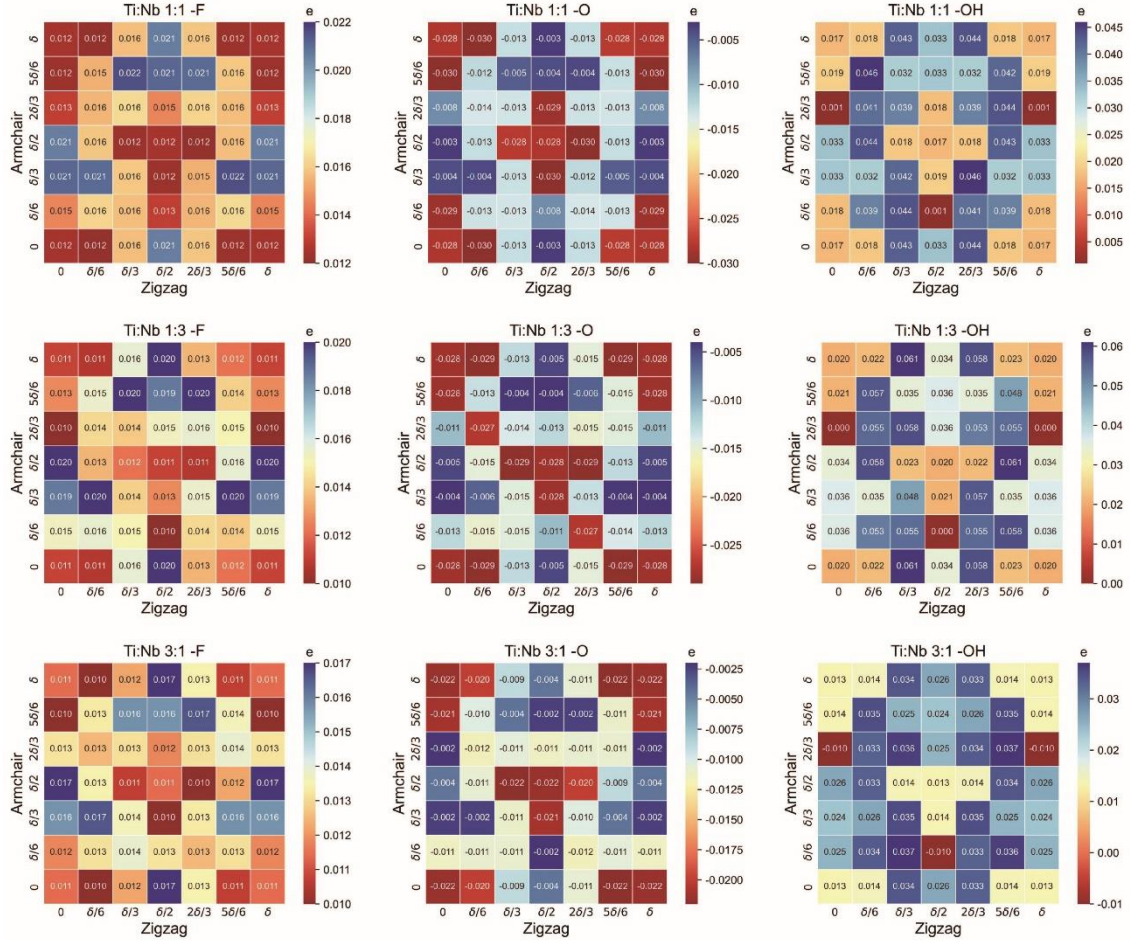


Supplementary Figure 9. Binding energy per area for heterostructures with various functional groups and layer-ratios.

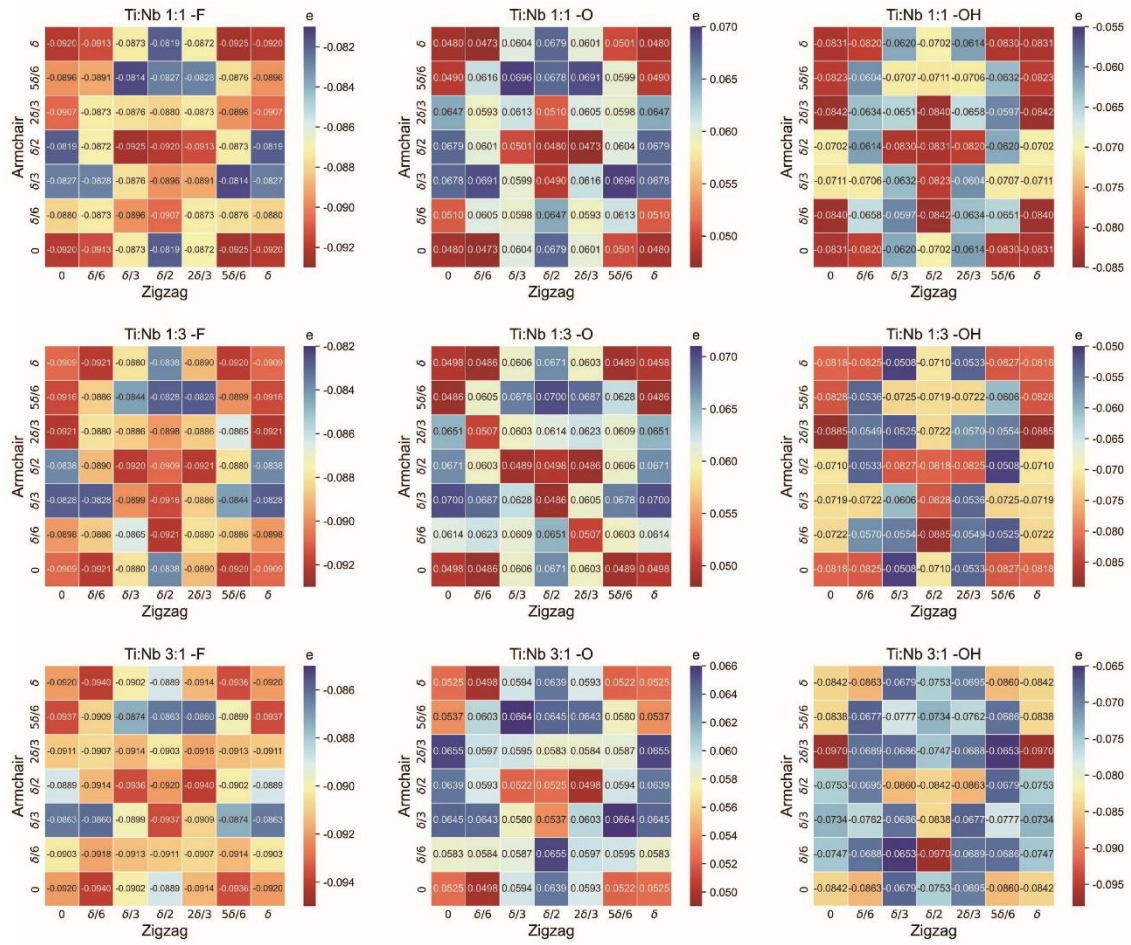
	Sliding barrier (meV)	Maximum Δd_{inter} (Å)
1Ti1Nb -F	86.451	0.628
1Ti1Nb -O	103.144	0.505
1Ti1Nb -OH	201.089	1.716
1Ti3Nb -F	86.776	0.606
1Ti3Nb -O	110.428	0.518
1Ti3Nb -OH	196.914	1.717
3Ti1Nb -F	79.852	0.573
3Ti1Nb -O	93.181	0.500
3Ti1Nb -OH	184.066	2.002

Supplementary Table 7. Sliding barriers and maximum interlayer spacing

enlargement for heterostructures with different layer ratios and terminations. The sliding barrier is taken from the global sliding. Δd_{inter} is the increase from the ground-state configuration to the maximum-energy configuration. Original data is provided in Supplementary Table 6.



Supplementary Figure 10. Charge transfer from Nb_2CT_x to $\text{Ti}_3\text{C}_2\text{T}_x$ of heterostructures with various functional groups and layer-ratios.

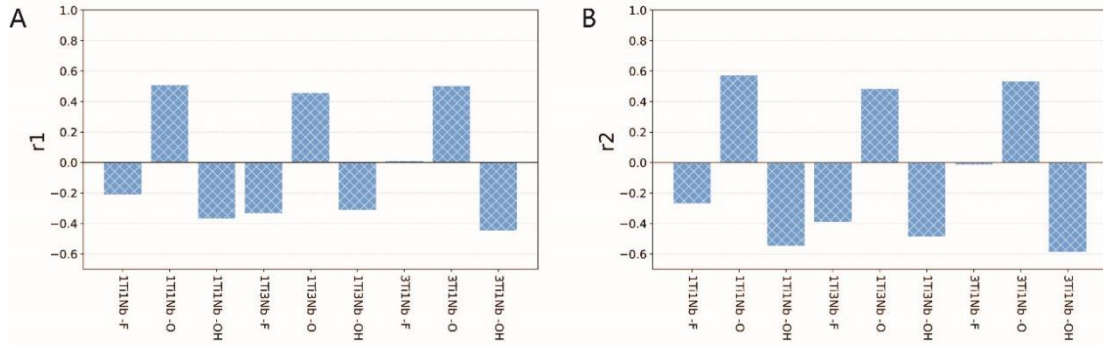


Supplementary Figure 11. Charge transfer from interlayer Nb&T_x to Ti&T_x of heterostructures with various functional groups and layer-ratios.

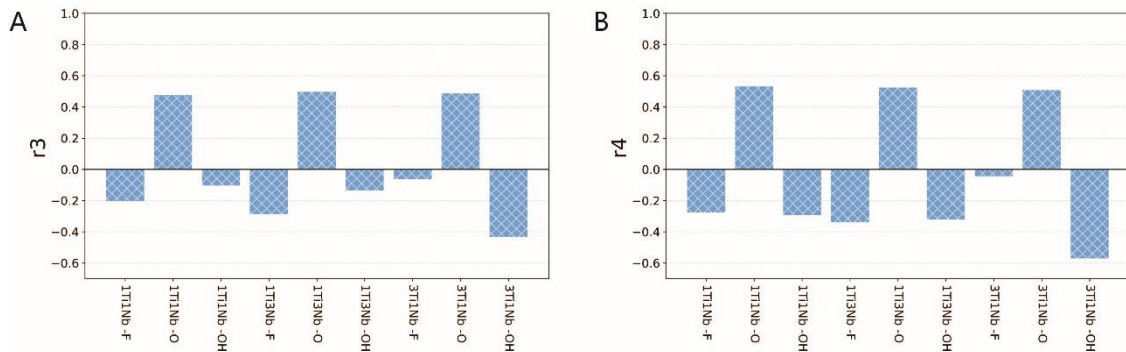
Models	r1	r2	r3	r4
1Ti1Nb -F	-0.2118	-0.2692	-0.2055	-0.2762
1Ti1Nb -O	0.5078	0.5727	0.476	0.5322
1Ti1Nb -OH	-0.3677	-0.5463	-0.1057	-0.2939
1Ti3Nb -F	-0.3327	-0.3903	-0.2872	-0.3399
1Ti3Nb -O	0.4565	0.4839	0.4972	0.5252
1Ti3Nb -OH	-0.3106	-0.4864	-0.1356	-0.3219
3Ti1Nb -F	0.0079	-0.0146	-0.0634	-0.0445
3Ti1Nb -O	0.5017	0.5312	0.4866	0.5084
3Ti1Nb -OH	-0.4469	-0.5865	-0.4337	-0.5723

Supplementary Table 8. The Pearson coefficients between charge transfer from

Nb_2CT_x to $\text{Ti}_3\text{C}_2\text{T}_x$ and systematic energy (r_1), between charge transfer from Nb_2CT_x to $\text{Ti}_3\text{C}_2\text{T}_x$ and d_{inter} (r_2), between interlayer charge transfer from ($\text{Nb}\&\text{T}_x$) to ($\text{Ti}\&\text{T}_x$) and systematic energy (r_3), between interlayer charge transfer from ($\text{Nb}\&\text{T}_x$) to ($\text{Ti}\&\text{T}_x$) and d_{inter} (r_4).



Supplementary Figure 12. (A) The Pearson coefficient (r_1) between charge transfer from Nb_2CT_x to $\text{Ti}_3\text{C}_2\text{T}_x$ and systematic energy; (B) The Pearson coefficient (r_2) between charge transfer from Nb_2CT_x to $\text{Ti}_3\text{C}_2\text{T}_x$ and d_{inter} . Original data is provided in Supplementary Table 8.



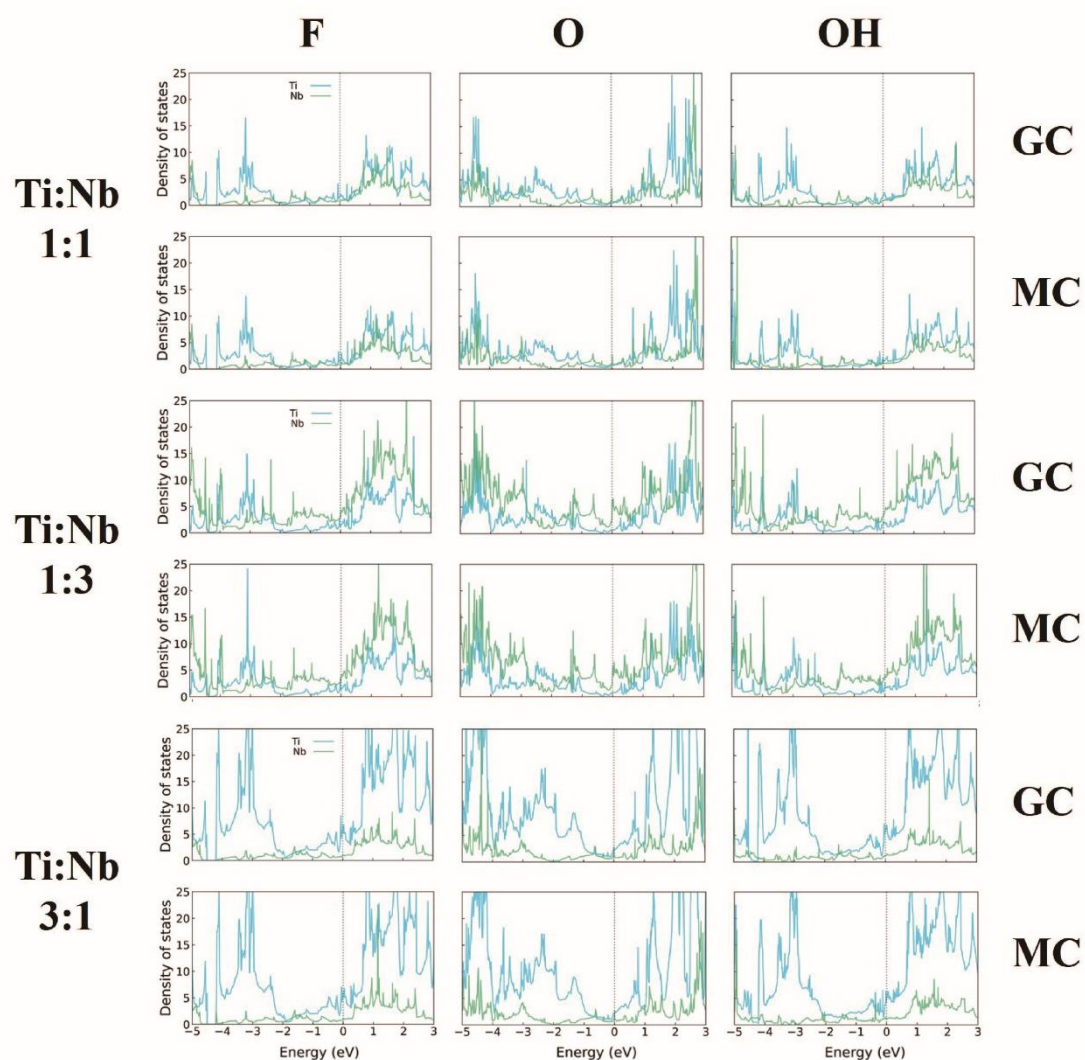
Supplementary Figure 13. (A) The Pearson coefficient (r_3) between interlayer charge transfer from ($\text{Nb}\&\text{T}_x$) to ($\text{Ti}\&\text{T}_x$) and systematic energy; (B) The Pearson coefficient (r_4) between interlayer charge transfer from ($\text{Nb}\&\text{T}_x$) to ($\text{Ti}\&\text{T}_x$) and d_{inter} . Original data is provided in Supplementary Table 8.

	1:1 -F	1:1 -O	1:1 -OH
R²	0.982	0.997	0.942

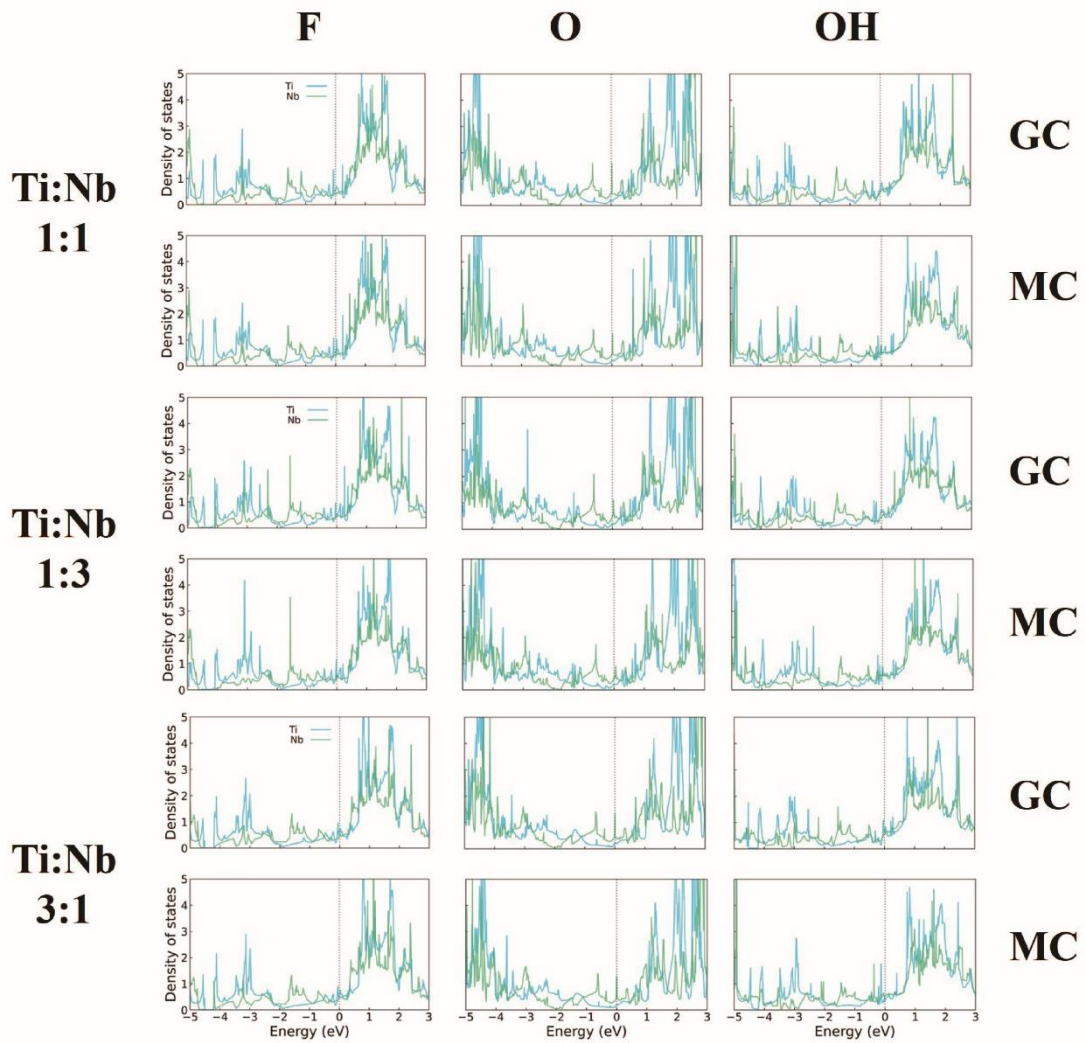
Supplementary Table 9. Coefficients of determination for varying functional groups between $-1/E_B$ and d_{inter}^6 using Ordinary Least Square for 1Ti1Nb.

	Energy/eV	DOS (Nb part)	DOS (Ti part)
1Ti1Nb -F Z0A5 (GC)	0.00534	0.81005	1.70385
1Ti1Nb -F Z0A4 (MC)	-0.0028	0.80462	1.63308
1Ti1Nb -O A0Z1 (GC)	-0.00294	0.96707	0.68951
1Ti1Nb -O Z0A4 (MC)	0.00138	0.96715	0.84243
1Ti1Nb -OH Z0A2 (GC)	0.00098	1.10462	1.94227
1Ti1Nb -OH Z0A4 (MC)	-0.00006	1.36554	1.861

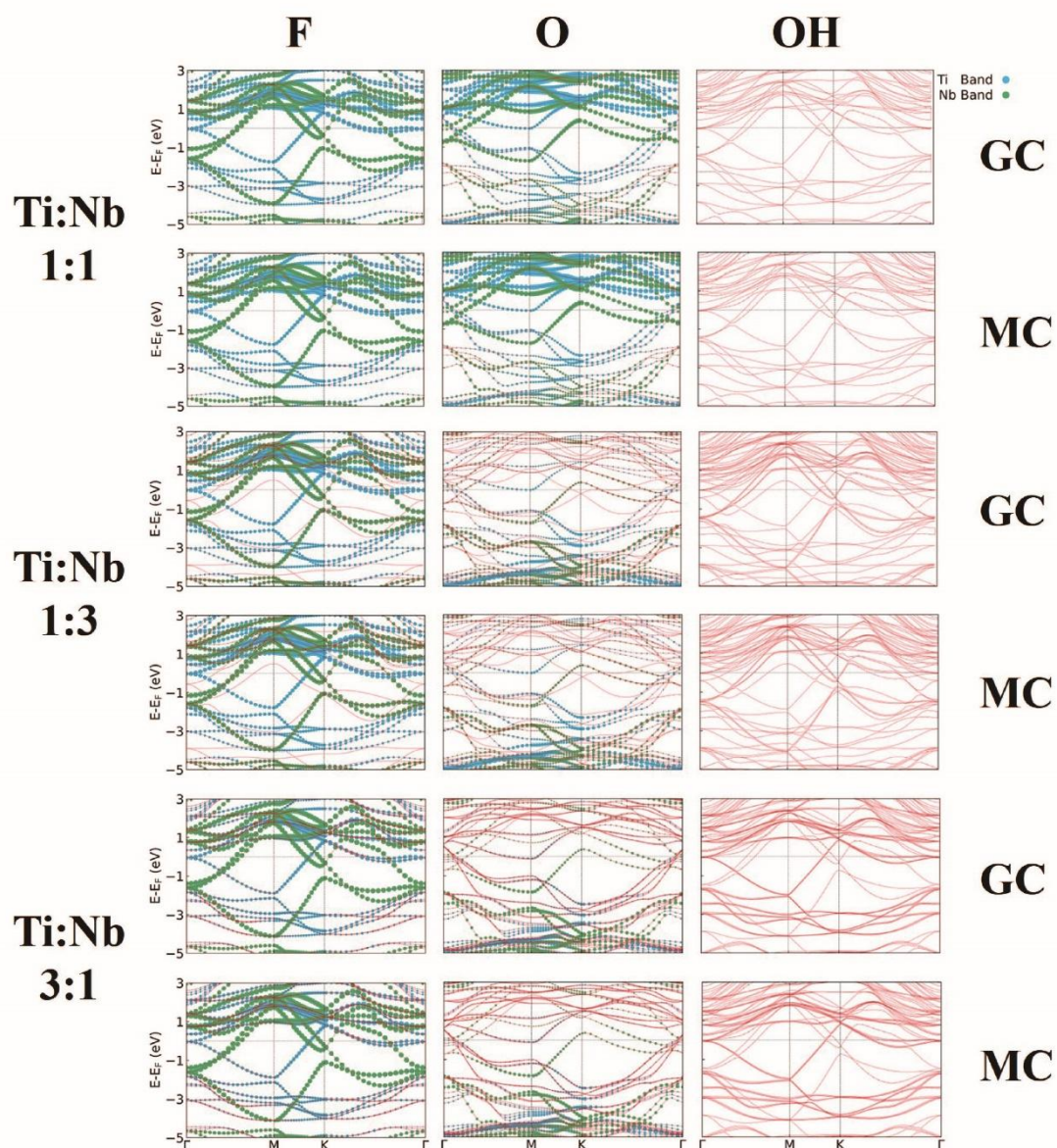
Supplementary Table 10. DOS values (at fermi level) of Nb_2CT_x and $\text{Ti}_3\text{C}_2\text{T}_x$ parts of the GCs and MCs of heterostructures with various functional groups and layer-ratios. DOS: Density of states; GCs: ground-state configurations; MCs: maximum-energy configurations.



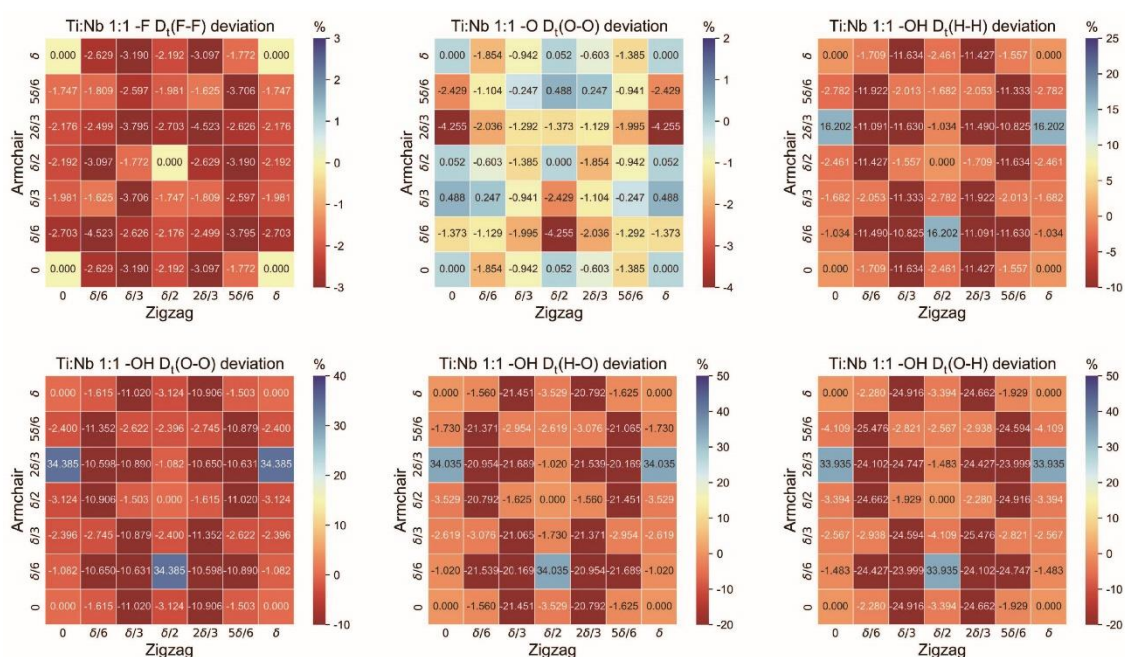
Supplementary Figure 14. DOS of Nb_2CT_x and $\text{Ti}_3\text{C}_2\text{T}_x$ parts of the GCs and MCs of heterostructures with various functional groups and layer-ratios. DOS values can be approached in Supplementary Table 10. DOS: Density of states; GCs: ground-state configurations; MCs: maximum-energy configurations.



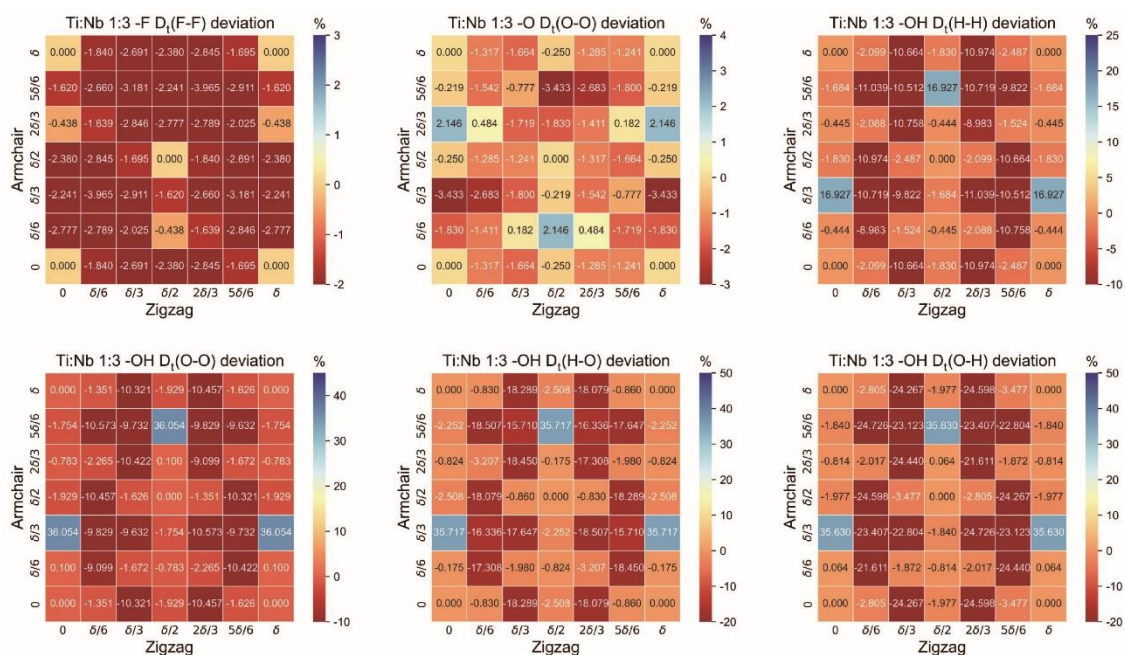
Supplementary Figure 15. LDOS of interlayer Nb&T_x and Ti&T_x of the GCs and MCs of heterostructures with various functional groups and layer-ratios. LDOS: Local density of states; GCs: ground-state configurations; MCs: maximum energies.



Supplementary Figure 16. Band of interlayer Nb&T_x and Ti&T_x of the GCs and MCs of heterostructures with various functional groups and layer-ratios. GCs: Ground-state configurations; MCs: maximum energies.

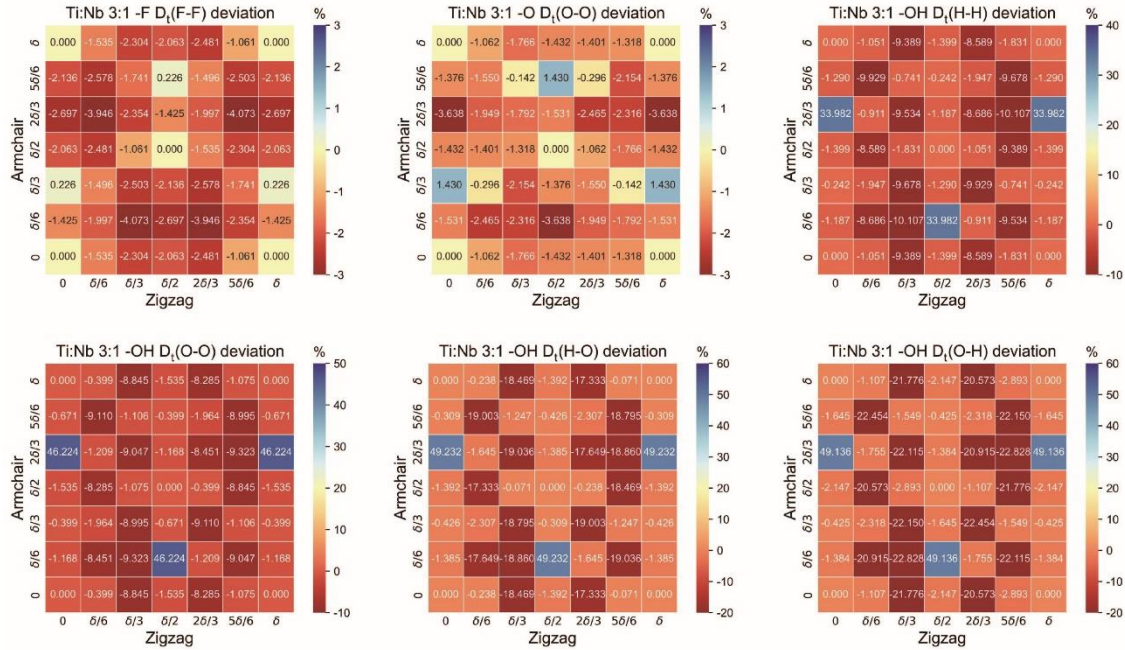


Supplementary Figure 17. The heat map of deviation of D_t values (the distance of nearest terminations sitting on separate sides at interspace) from corresponding values of initial 1Ti1Nb heterostructure. H-O means H atoms in $Ti_3C_2T_x$ parts and O atoms in Nb_2CT_x parts, while O-H means O atoms in $Ti_3C_2T_x$ parts and H atoms in Nb_2CT_x parts.

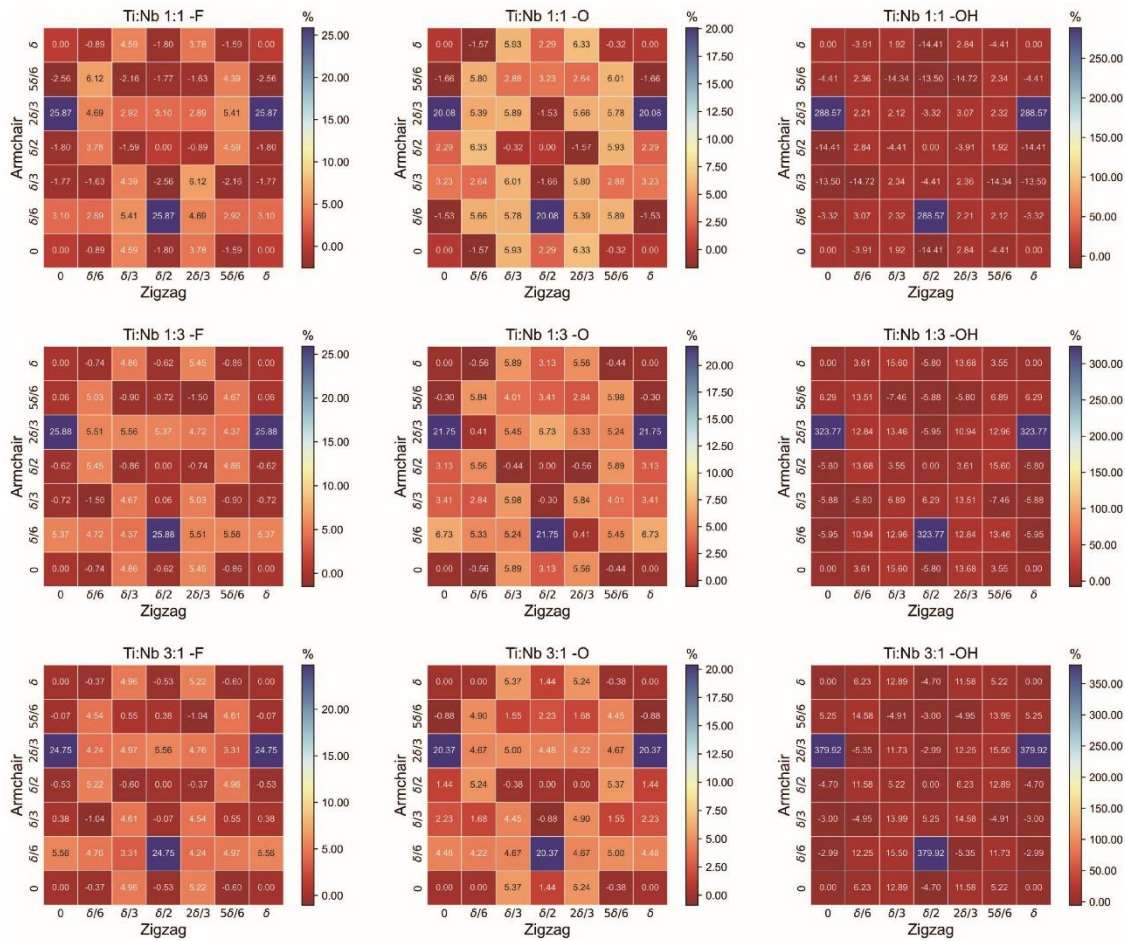


Supplementary Figure 18. The heat map of deviation of D_t values (the distance of

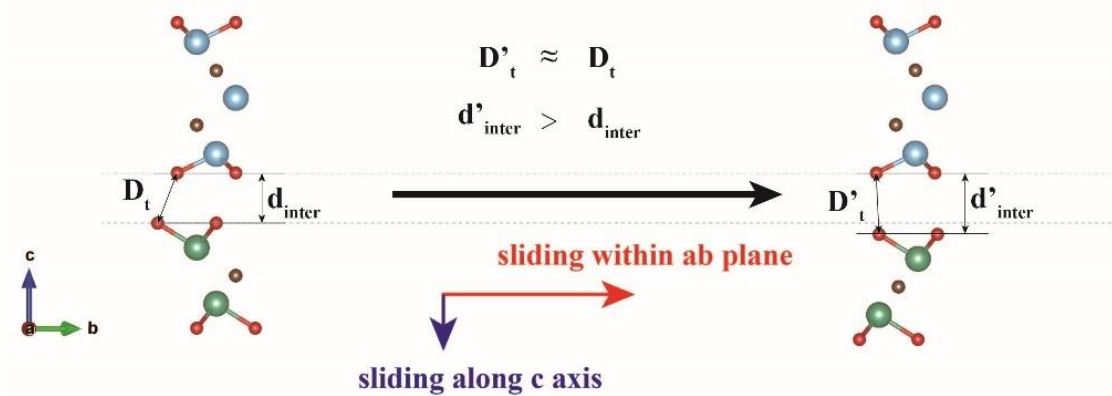
nearest terminations sitting on separate sides at interspace) from corresponding values of initial 1Ti3Nb heterostructure. H-O means H atoms in $Ti_3C_2T_x$ parts and O atoms in Nb_2CT_x parts, while O-H means O atoms in $Ti_3C_2T_x$ parts and H atoms in Nb_2CT_x parts.



Supplementary Figure 19. The heat map of deviation of D_t values (the distance of nearest terminations sitting on separate sides at interspace) from corresponding values of initial 3Ti1Nb heterostructure. H-O means H atoms in $Ti_3C_2T_x$ parts and O atoms in Nb_2CT_x parts, while O-H means O atoms in $Ti_3C_2T_x$ parts and H atoms in Nb_2CT_x parts.

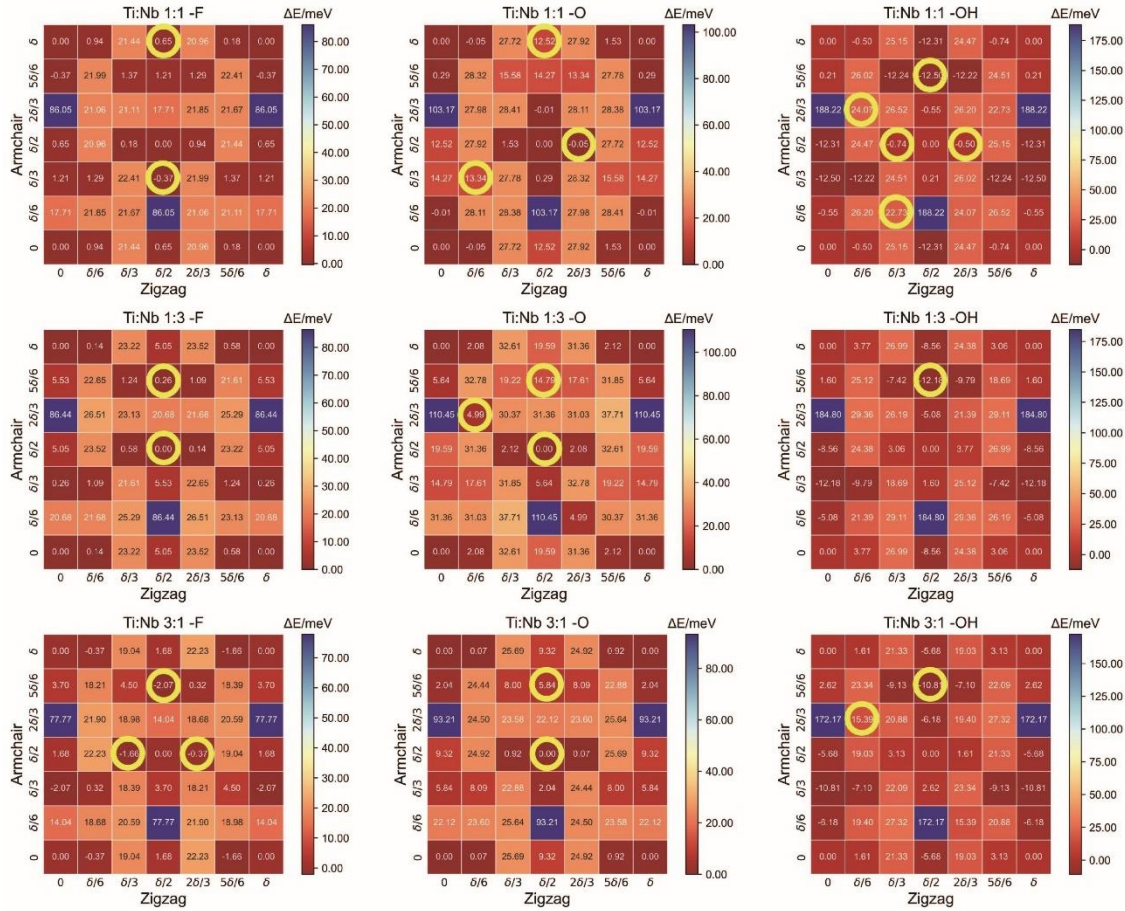


Supplementary Figure 20. Full-period interlayer distance variation scales comparing with initial heterostructures, for configurations with various functional groups and layer-ratios.

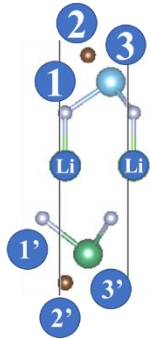


Supplementary Figure 21. Schematic of the decoupled interlayer correlation during sliding in $-F/-O$ MXene heterostructures. $1Ti1Nb$ $-O$ sliding from GC to MC is showing as an example here, the Nb_2CO_2 monolayer slides not only within ab plane but

also along c axis, resulting an enlarged d_{inter} with a nearly constant D_t .



Supplementary Figure 22. Full-period systematic energy variation amplitude comparing with initial heterostructures, for configurations with various functional groups and layer-ratios. The local energy minima are indicated with gold circles.



	Min Li 1	Min Na 1	Min Li 2	Min Na 2	Max Li 1	Max Na 1	Max Li 2	Max Na 2
1:1 -F	2, d	2', d	1, 2, d	2', 2	1, d	/, d	1, 2, d	/, 2 (2'), d
1:1 -O	2	2	2', 2	2, 2	2	2 (2')	2', 2	2 (2'), 2 (2')
1:1 -OH	3 (2')	3 (2')	2', 2	2', 2	2 (2')	2 (2')	2 (2'), 3	2 (2'), 3
1:3 -F	2', d	2, d	2', 2, d	2, 2, d	2 (2'), d	2 (2'), d	2 (2'), 3, d	2 (2'), 2 (2'), d
1:3 -O	2	2	2, 2	2, 2	2 (2')	2 (2')	2 (2'), 2 (2')	2 (2'), 2 (2')
1:3 -OH	3 (2')	3 (2')	2', 2	2', 2	2 (2')	2 (2')	2 (2'), 3	2 (2'), 3
3:1 -F	2 (2'), d	2, d	2(2'), /, d	2, 1', d	2 (2'), d	2 (2')	2 (2'), 3, d	2 (2'), 2 (2'), d
3:1 -O	2	2	2, 2	2, 2	2 (2')	2 (2')	2 (2'), 2 (2')	2 (2'), 2 (2')
3:1 -OH	3 (2')	3 (2')	2', 2	2', 2	2 (2')	2 (2')	2 (2'), 3	2 (2'), 3

Supplementary Table 11. The statistics of intercalated Li/Na atoms' ground-state positions after relaxation. "min Li 1" means 1L Li intercalation in ground-state configurations, "max Na 2" means 2L Na Intercalation in maximum-energy configurations, and so on. Numbers 1, 2 and 3 represents the a-b plane coordination of functional groups, C atoms and Ti atoms in $Ti_3C_2T_x$ near interspace, while 1', 2' and 3' represents positions of corresponding atoms in Nb_2CT_x . Symbols '/' and 'd' means that Li/Na atoms align with none of six positions, and distortion arises due to bonds formation between terminations and Li/Na, respectively.

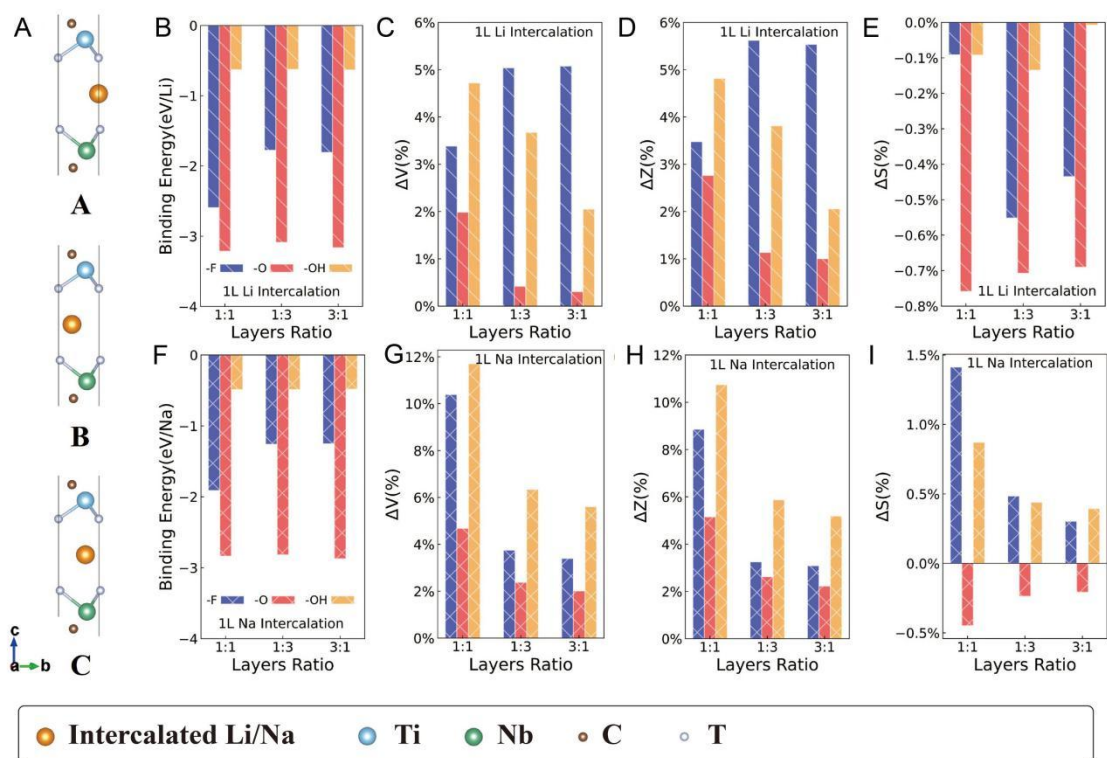
Max 1-layer Li Binding Energy (eV/Li)			
	1Ti1Nb	1Ti3Nb	3Ti1Nb
F	-2.5911	-1.7748	-1.8054
O	-3.2124	-3.0862	-3.1616
OH	-0.6264	-0.6234	-0.6306

Max 2-layer Li Binding Energy (eV/Li)			
	1Ti1Nb	1Ti3Nb	3Ti1Nb
F	-1.8309	-1.6860	-1.7072
O	-2.0065	-1.9808	-2.0190
OH	-0.5694	-0.5681	-0.5666

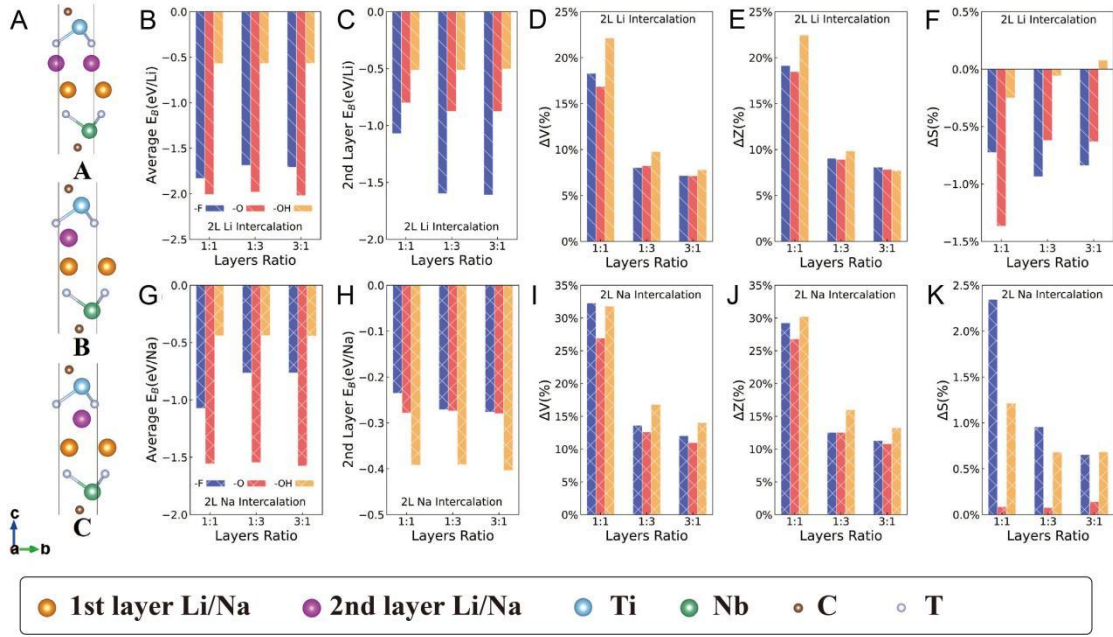
Max 1-layer Na Binding Energy (eV/Na)			
	1Ti1Nb	1Ti3Nb	3Ti1Nb
F	-1.9090	-1.2578	-1.2509
O	-2.8348	-2.8164	-2.8718
OH	-0.4863	-0.4862	-0.4803

Max 2-layer Na Binding Energy (eV/Na)			
	1Ti1Nb	1Ti3Nb	3Ti1Nb
F	-1.0722	-0.7643	-0.7638
O	-1.5565	-1.5451	-1.5757
OH	-0.4391	-0.4384	-0.4420

Supplementary Table 12. E_B per Li/Na atom for 1L and 2L alkali intercalation in maximum-energy configurations. More detailed data of other models are accessible in supplementary excel “Li, Na Intercalation Data”.



Supplementary Figure 23. (A) Schematic diagrams for MCs intercalated by Li at high-symmetry sites A, B and C, respectively, orange balls represent Li/Na atoms. Ground states mostly exhibit in sites B (or A) which locate upon C atoms; (B) E_B per Li atom for 1L Li intercalation; (C) ΔV , (D) ΔZ and (E) ΔS for 1L Li intercalation; (F) E_B per Na atom for 1L Na intercalation; (G) ΔV , (H) ΔZ and (I) ΔS for 1L Na intercalation. Figure (B-E) share the same legend, and so do Figure (F-I). Original data is provided in Supplementary Table 12.

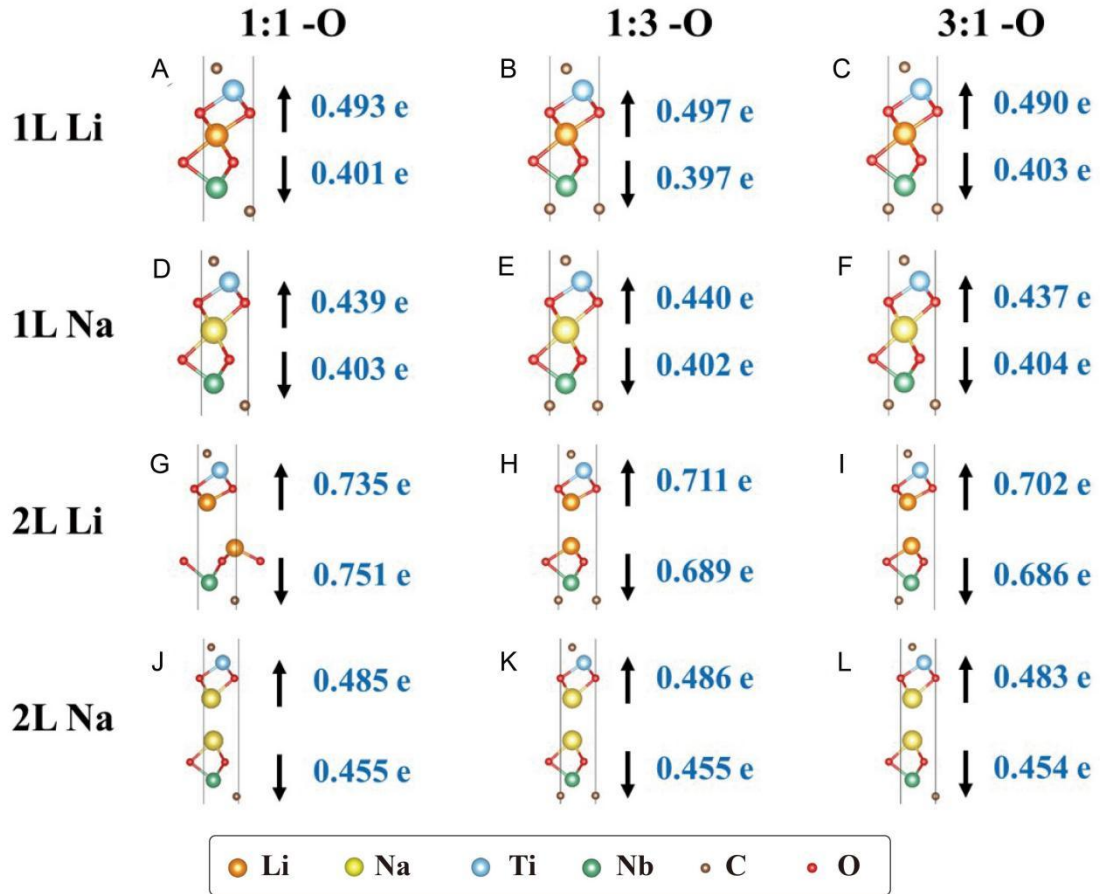


Supplementary Figure 24. (A) Schematic diagrams for MCs intercalated by 2L Li/Na, in which the 2nd layer Li/Na atoms locate at high-symmetry sites A, B and C, respectively, orange balls represent the 1st layer Li/Na atoms, and pink balls represent the 2nd layer Li/Na atoms. Ground states mostly exhibit in sites B (or A) locating upon C atoms; (B) E_B per Li atom for 2L Li intercalation; (C) E_B per Li atom of the 2nd layer intercalated Li; (D) ΔV , (E) ΔZ and (F) ΔS for 2L Li intercalation; (G) E_B per Na atom for 2L Na intercalation; (H) E_B per Na atom of the 2nd layer intercalated Na; (I) ΔV , (J) ΔZ and (K) ΔS for 2L Na intercalation. Figure (B-F) share the same legend, and so do Figure (G-K). Original data is provided in Supplementary Table 12.

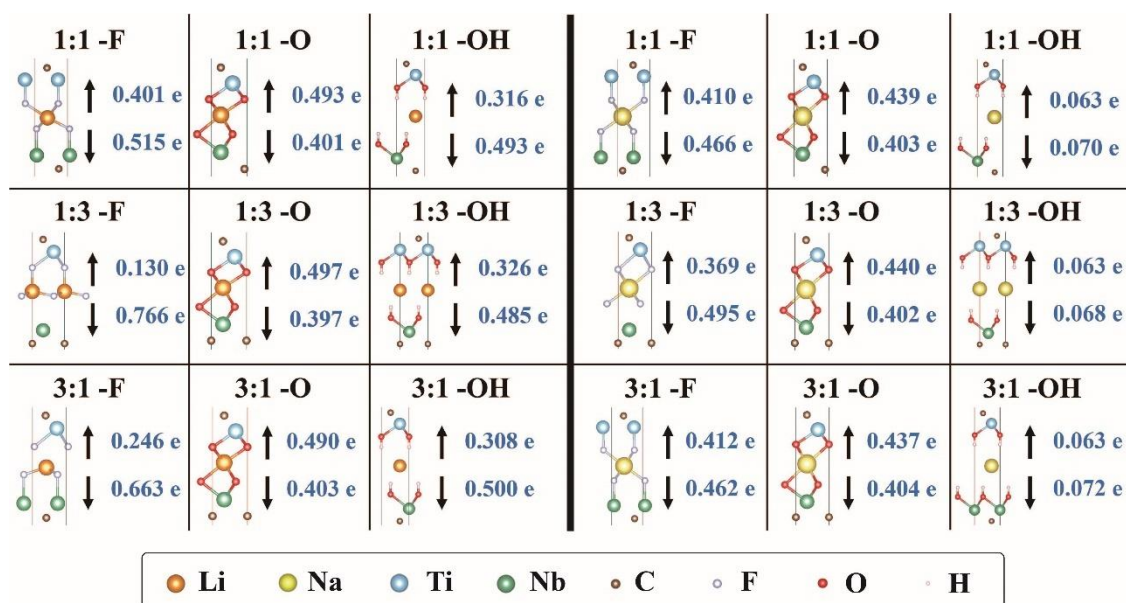
	1L Li (mAh/g)	2L Li (mAh/g)	1L Na (mAh/g)	2L Na (mAh/g)
1Ti1Nb -F*	59.77	117.72	57.70	109.97
1Ti1Nb -O*	61.41	120.90	59.24	112.74
1Ti1Nb -OH*	60.85	119.81	58.71	111.79
1Ti3Nb -F*	29.13	57.82	28.63	55.89
1Ti3Nb -O*	29.91	59.36	29.38	57.32
1Ti3Nb -OH*	29.64	58.83	29.13	56.83
3Ti1Nb -F*	31.18	61.85	30.60	59.64
3Ti1Nb -O*	32.07	63.61	31.47	61.28

3Ti1Nb -OH*	31.77	63.01	31.17	60.72
Ti ₂ CO ₂ ^[4]	348		288	
V ₂ CO ₂ ^[4]	335		279	
Nb ₂ CO ₂ ^[4]	219		194	
Ti ₃ C ₂ O ₂ ^[4]	250		217	
Ti ₂ C ^[4]	439		348	
V ₂ C ^[4]	418		335	
Nb ₂ C ^[4]	252		219	
Ti ₃ C ₂ ^[4]	294		250	
Ti ₂ C(OH) ₂ ^[5]	344.397			
Ti ₂ CO ₂ ^[5]	348.926			
V ₂ CO ₂ ^[5]	335.495			
V ₂ C(OH) ₂ ^[5]	331.306			

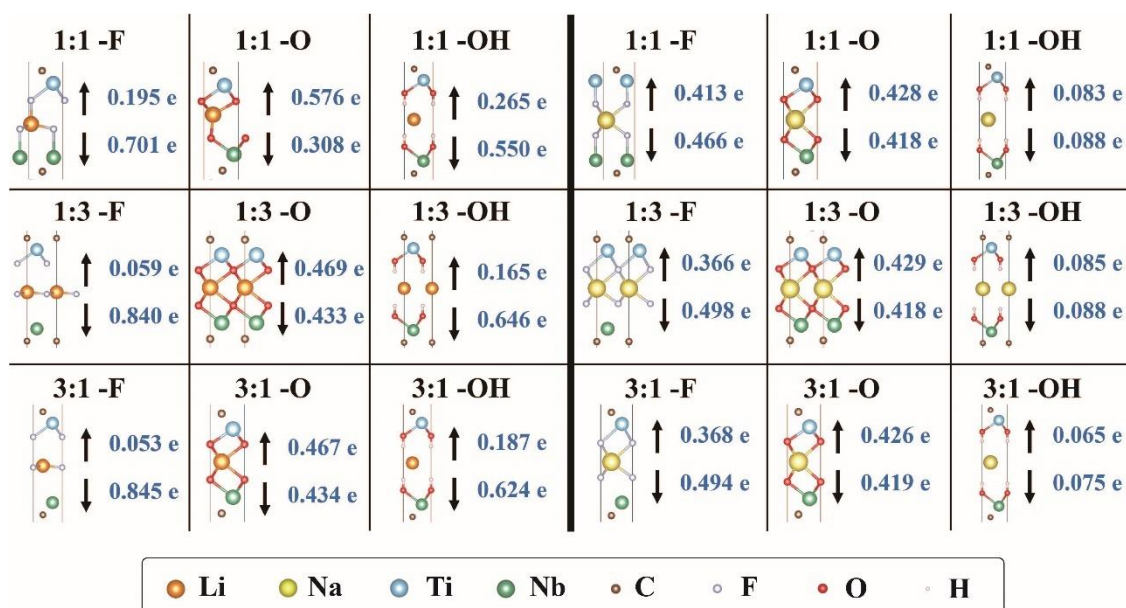
Supplementary Table 13. Theoretical metal ion capacities (mAh/g) corresponding to one or two metal layers intercalated in the interlayer of MXene heterostructures in comparison with previously reported data from the literature. Rows with * are data calculated in this work.



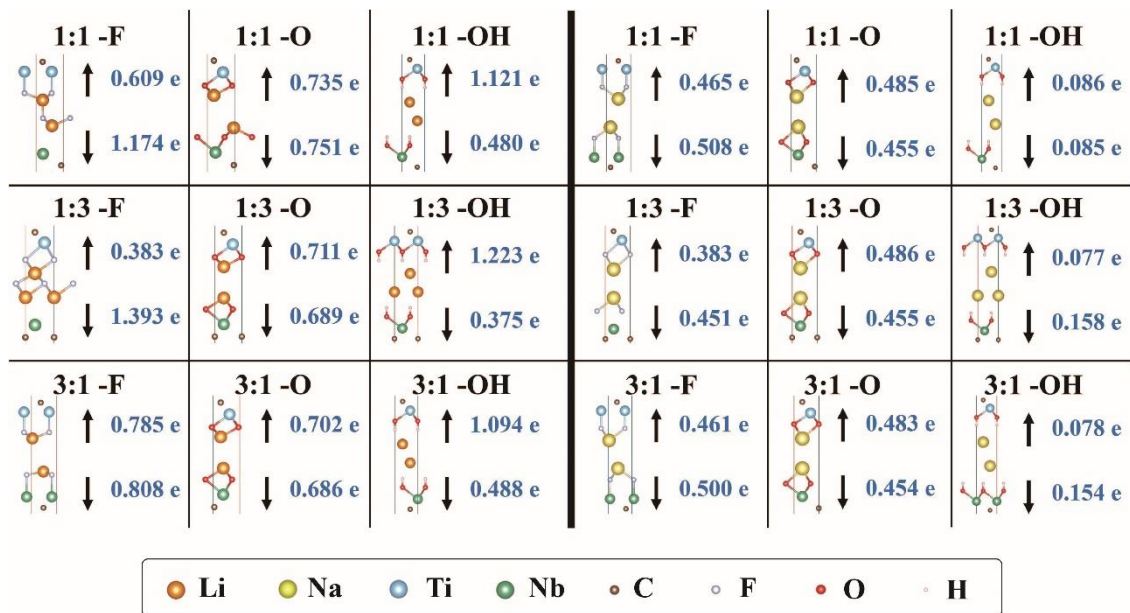
Supplementary Figure 25. Charge transfer of alkali atoms to $\text{Ti}_3\text{C}_2\text{T}_x$ parts (upward arrows) and Nb_2CT_x parts (downward arrows) for -O terminated ground-state configurations (the most stable configurations among various terminations). (A-C) show charge transfer of 1L Li intercalation in -O terminated MXene with various layer-ratios; (D-F) show charge transfer of 1L Na intercalation in -O terminated MXene with various layer-ratios; (G-I) show charge transfer of 2L Li intercalation in -O terminated MXene with various layer-ratios; (J-I) show charge transfer of 2L Na intercalation in -O terminated MXene with various layer-ratios. Li, Na atoms are denoted by orange and gold balls in the interlayer.



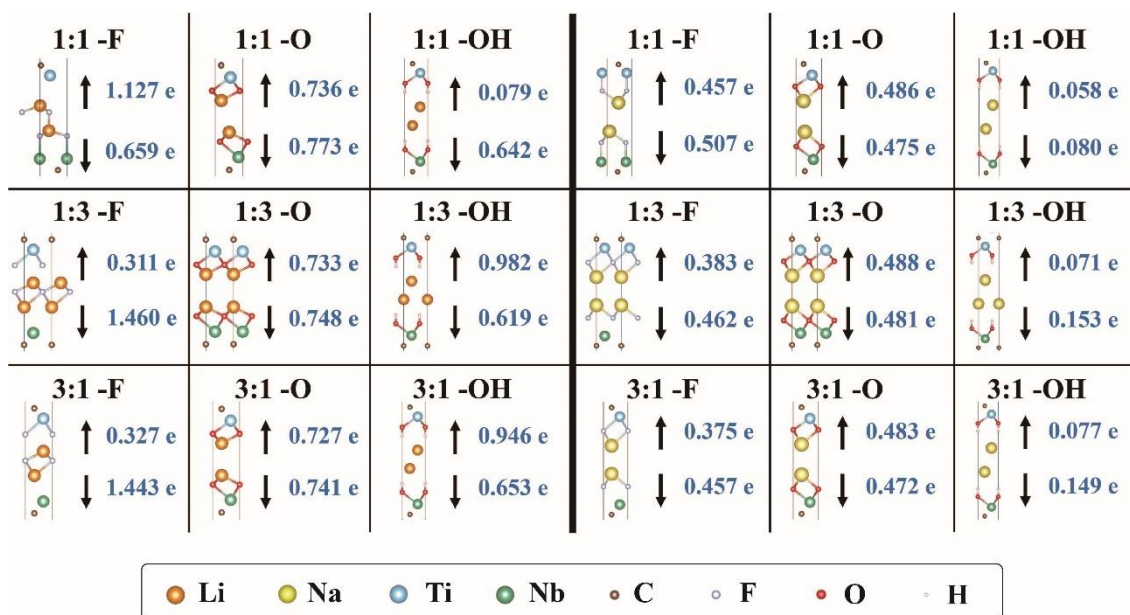
Supplementary Figure 26. Charge transfer of alkali atoms to $\text{Ti}_3\text{C}_2\text{T}_x$ parts (upward arrows) and Nb_2CT_x parts (downward arrows) for 1L intercalation in GCs, the left (right) panel shows Li (Na) intercalation, Li (Na) atoms are denoted by orange (gold) balls in the interlayer.



Supplementary Figure 27. Charge transfer of alkali atoms to $\text{Ti}_3\text{C}_2\text{T}_x$ parts (upward arrows) and Nb_2CT_x parts (downward arrows) for 1L intercalation in MCs, the left (right) panel shows Li (Na) intercalation, Li (Na) atoms are denoted by orange (gold) balls in the interlayer.

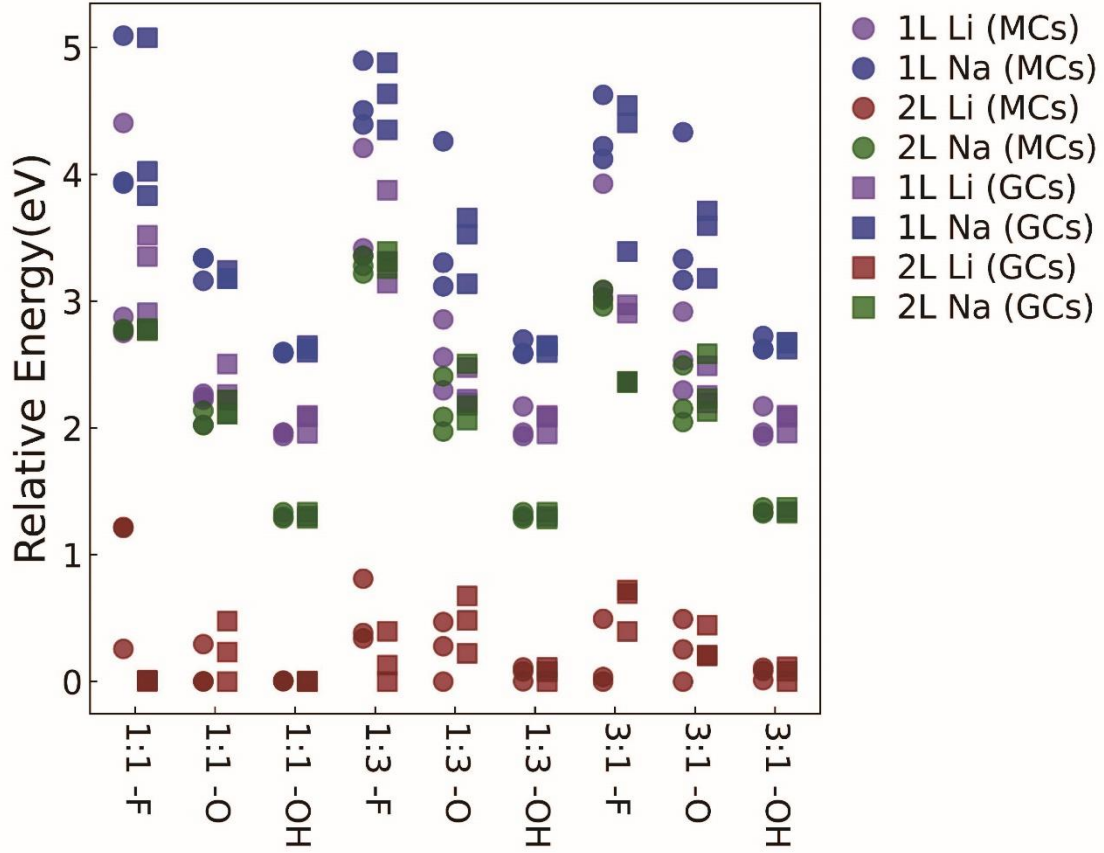


Supplementary Figure 28. Charge transfer of alkali atoms to $\text{Ti}_3\text{C}_2\text{T}_x$ parts (upward arrows) and Nb_2CT_x parts (downward arrows) for 2L intercalation in GCs, the left (right) panel shows Li (Na) intercalation, Li (Na) atoms are denoted by orange (gold) balls in the interlayer.



Supplementary Figure 29. Charge transfer of alkali atoms to $\text{Ti}_3\text{C}_2\text{T}_x$ parts (upward arrows) and Nb_2CT_x parts (downward arrows) for 2L intercalation in MCs, the left (right) panel shows Li (Na) intercalation, Li (Na) atoms are denoted by orange (gold) balls in the interlayer.

balls in the interlayer.



Supplementary Figure 30. Relative systematic energies of heterostructures after Li/Na intercalation in three high-symmetry sites, the lowest energy among structures with specific layer-ratio and termination is set to be 0 as the reference.

	Y^{2D}_x (N/m)	Y^{2D}_y (N/m)	Y^{2D} (N/m)
$Ti_2C^{[6]}$	143	144	
$Ti_2CO_2^{[6]}$	248	250	
$Ti_2CF_2^{[6]}$	138	140	
$Ti_2C(OH)_2^{[6]}$	160	162	
$Ti_3C_2^{[6]}$	247	251	
$Ti_3C_2O_2^{[6]}$	366	372	
$Ti_3C_2F_2^{[6]}$	302	303	

$\text{Ti}_3\text{C}_2(\text{OH})_2^{[6]}$	316	319	
$\text{Ti}_4\text{C}_3^{[6]}$	305	298	
$\text{Ti}_4\text{C}_3\text{O}_2^{[6]}$	490	488	
$\text{Ti}_4\text{C}_3\text{F}_2^{[6]}$	437	436	
$\text{Ti}_4\text{C}_3(\text{OH})_2^{[6]}$	420	422	
$\text{Ti}_3\text{C}_2^{[7]}$	313	312	
$\text{Ti}_3\text{C}_2\text{O}_2^{[7]}$	368	369	
$\text{Ti}_3\text{C}_2\text{F}_2^{[7]}$	312	309	
$\text{Ti}_3\text{C}_2(\text{OH})_2^{[7]}$	262	267	
$\text{Ti}_2\text{C}^{[8]}$			135.53
$\text{Ti}_2\text{CO}_2^{[8]}$			241.86
$\text{Ti}_2\text{CF}_2^{[8]}$			136.67
$\text{Ti}_2\text{C}(\text{OH})_2^{[8]}$			179.12
$\text{Nb}_2\text{C}^{[8]}$			178.13
$\text{Nb}_2\text{CO}_2^{[8]}$			281.65
$\text{Ti}_3\text{C}_2^{[8]}$			214.85
$\text{Ti}_3\text{C}_2\text{O}_2^{[8]}$			361.42
$\text{Ti}_3\text{C}_2\text{F}_2^{[8]}$			271.93
$\text{Ti}_3\text{C}_2(\text{OH})_2^{[8]}$			266.05
$\text{Nb}_4\text{C}_3^{[8]}$			402.59
$\text{Nb}_4\text{C}_3\text{O}_2^{[8]}$			605.99
$\text{Nb}_4\text{C}_3\text{F}_2^{[8]}$			466.38
$\text{Nb}_4\text{C}_3(\text{OH})_2^{[8]}$			497.97
$\text{MoS}_2^{[8]}$			123
Graphene ^[8]			335
Graphene ^[9]			328.76
h-BN ^[9]			282.03
h-MoS ₂ ^[9]			140.59
$\text{Ti}_2\text{C}^{[9]}$			143.16

Ti ₂ CO ₂ ^[9]		248.38
Ti ₃ C ₂ ^[9]		246.01
Ti ₃ C ₂ O ₂ ^[9]		328.64
Ti ₄ C ₃ ^[9]		338.58
Ti ₄ C ₃ O ₂ ^[9]		470.36
1Ti1Nb -F*	445.75	436.46
1Ti1Nb -O*	575.28	583.69
1Ti1Nb -OH*	467.15	452.39
1Ti3Nb -F*	804.47	782.55
1Ti3Nb -O*	1139.48	1142.99
1Ti3Nb -OH*	912.96	922.13
3Ti1Nb -F*	1022.44	1006.82
3Ti1Nb -O*	1260.65	1236.93
3Ti1Nb -OH*	1097.27	1076.87

Supplementary Table 14. Calculated in-plane Youngs moduli of the 2D ground state structures with various terminations and layer-ratios in comparison with previously reported data from the literature, where 1Ti1Nb means heterostructure constructed by 1 layer of Ti₃C₂T_x monolayer and 1 layer of Nb₂CT_x monolayer. Rows with * are data calculated in this work. Original data is provided in Supplementary Table 15.

	C11	C22	C12	C21	C66	v^{2D}(xy)	v^{2D}(yx)	Y^{2D}(x)	Y^{2D}(y)	G^{2D}(yx)
	(N/m)	(N/m)	(N/m)	(N/m)	(N/m)))	(N/m)	(N/m)	(N/m)
1Ti1Nb -F	486.118	475.986	138.623	138.623	176.879	0.291	0.285	445.746	436.456	176.879
1Ti1Nb -O	632.134	641.368	190.952	190.952	225.764	0.298	0.302	575.283	583.686	225.764
1Ti1Nb -OH	503.839	487.923	133.806	133.806	194.697	0.274	0.266	467.145	452.388	194.697
1Ti3Nb -F	898.778	874.290	287.147	287.147	313.882	0.328	0.319	804.469	782.551	313.882
1Ti3Nb -O	1253.707	1257.566	379.007	379.007	445.096	0.301	0.302	1139.482	1142.989	445.096
1Ti3Nb -OH	965.239	974.936	225.770	225.770	357.924	0.232	0.234	912.957	922.128	357.924
3Ti1Nb -F	1112.322	1095.329	313.766	313.766	435.970	0.286	0.282	1022.441	1006.822	435.970
3Ti1Nb -O	1392.955	1366.740	425.234	425.234	493.370	0.311	0.305	1260.652	1236.926	493.370
3Ti1Nb -OH	1169.206	1147.471	287.310	287.310	437.213	0.250	0.246	1097.268	1076.870	437.213

Supplementary Table 15. The in-plane Young's modulus (Y^{2D}), shear modulus (G^{2D}), and Poisson's ratio (v^{2D}) of the 2D ground state structures, calculated using energy-strain method.

	From T to Ti (e)		From T to Nb (e)	
	at interlayer	near vacuum	at interlayer	near vacuum
1Ti1Nb -F Z0A5	-0.7603	-0.7575	-0.7430	-0.7429
1Ti1Nb -O A0Z1	-1.1088	-1.1035	-1.1174	-1.1073
1Ti1Nb -OH Z0A2	-0.7346	-0.7490	-0.7080	-0.7623
1Ti3Nb -F A0Z5	-0.7182	-0.7568	-0.7449	-0.7414
1Ti3Nb -O A0Z0	-1.0740	-1.1101	-1.0974	-1.1071
1Ti3Nb -OH Z0A4	-0.7356	-0.7473	-0.7241	-0.7609
3Ti1Nb -F Z0A2	-0.7567	-0.7541	-0.7378	-0.7404
3Ti1Nb -O A0Z0	-1.0988	-1.1012	-1.1080	-1.0992
3Ti1Nb -OH Z0A2	-0.7310	-0.7493	-0.7094	-0.7641

Supplementary Table 16. Charge transfer from T (-F, -O, -OH) to M (Ti, Nb) of 2D ground state configurations.

Appendix I

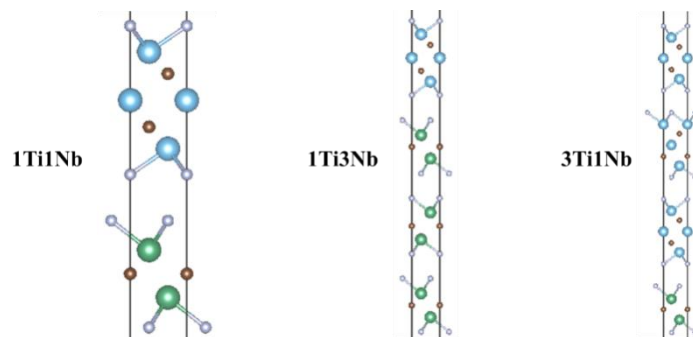
The POSCAR and CONTCAR figures of 18 $Ti_3C_2T_x/Nb_2CT_x$ heterostructures on the top and bottom, respectively, with systematic (unit: eV, omitted in lists) listed orderly.

For conciseness, only atoms at interspace are displayed.

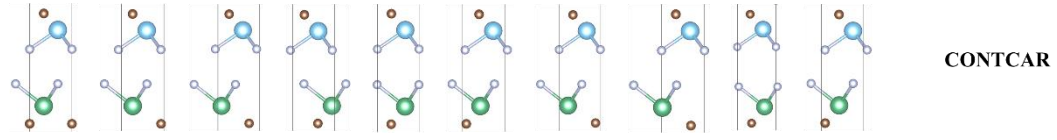
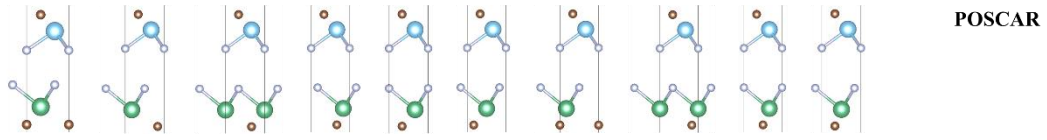
The legends in appendix I are uniformly provided as follows:



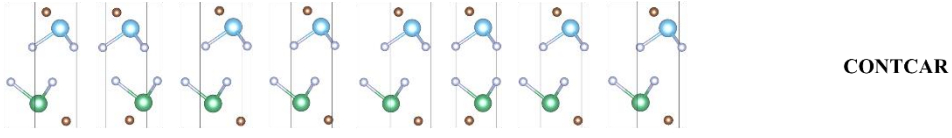
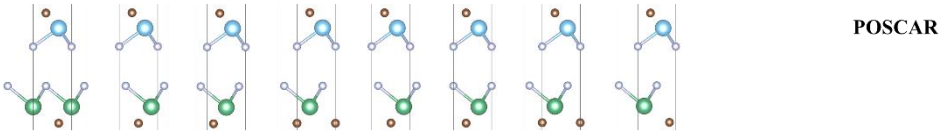
Atomic structural schematic of AM_0ZZ_0 configurations of different layer-ratios (termination: -F)



1Ti1Nb -F

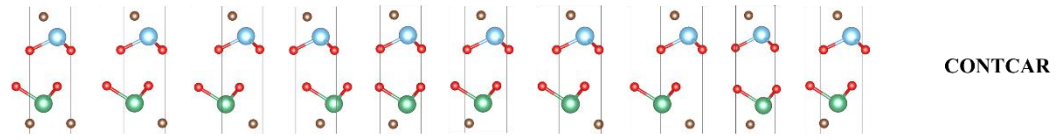
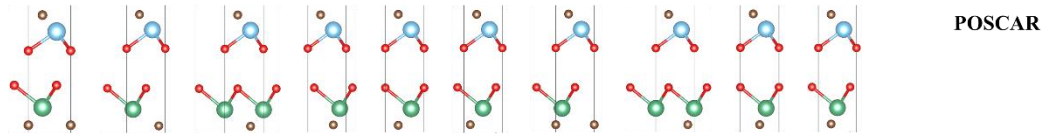


AM ₀ ZZ ₀	AM ₇ ZZ _{0/6}	AM ₁ ZZ _{0/3}	AM ₇ ZZ _{0/2}	AM ₉ ZZ _{20/3}	AM ₇ ZZ _{50/6}	AM _{8/7} ZZ ₀	AM _{0/3} ZZ ₀	AM _{20/3} ZZ ₀	AM _{50/6} ZZ ₀
-101.430eV	-101.429eV	-101.408eV	-101.429eV	-101.409eV	-101.430eV	-101.412eV	-101.429eV	-101.344eV	-101.430eV

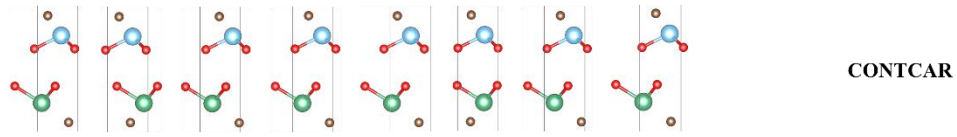
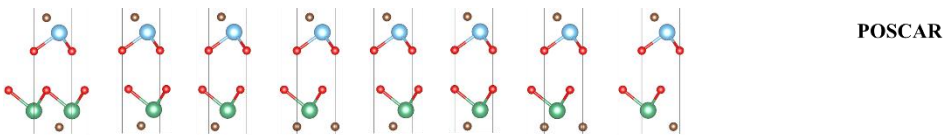


AM _{0/6} ZZ _{0/6}	AM _{0/3} ZZ _{0/6}	AM _{20/3} ZZ _{0/6}	AM _{50/6} ZZ _{0/6}	AM _{0/6} ZZ _{0/3}	AM _{0/3} ZZ _{0/3}	AM _{20/3} ZZ _{0/3}	AM _{50/6} ZZ _{0/3}
-101.408eV	-101.429eV	-101.409eV	-101.408eV	-101.408eV	-101.407eV	-101.409eV	-101.428eV

1Ti1Nb -O

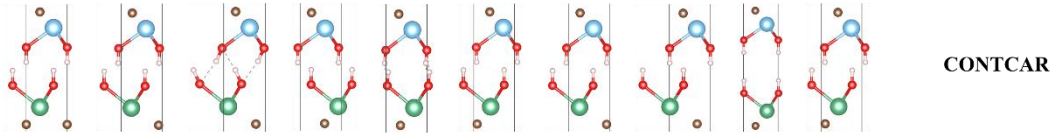
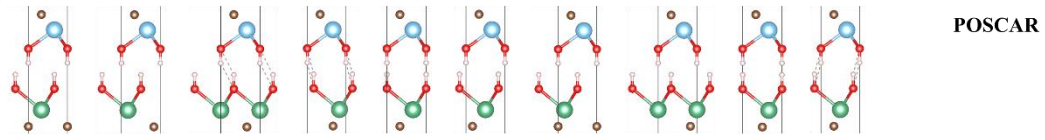


AM ₀ ZZ ₀	AM ₇ ZZ _{0/6}	AM ₀ ZZ _{0/3}	AM ₇ ZZ _{0/2}	AM ₉ ZZ _{20/3}	AM ₇ ZZ _{50/6}	AM _{8/7} ZZ ₀	AM _{0/3} ZZ ₀	AM _{20/3} ZZ ₀	AM _{50/6} ZZ ₀
-112.767eV	-112.768eV	-112.740eV	-112.755eV	-112.740eV	-112.766eV	-112.767eV	-112.753eV	-112.664eV	-112.767eV

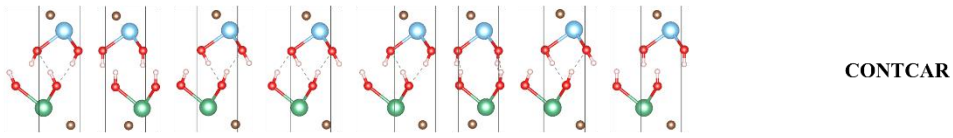
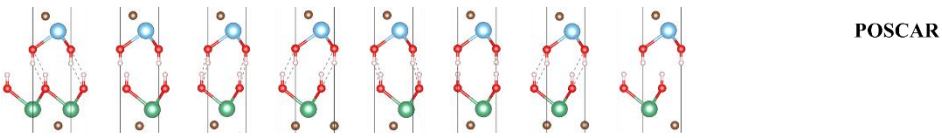


AM _{0/6} ZZ _{0/6}	AM _{0/3} ZZ _{0/6}	AM _{20/3} ZZ _{0/6}	AM _{50/6} ZZ _{0/6}	AM _{0/6} ZZ _{0/3}	AM _{0/3} ZZ _{0/3}	AM _{20/3} ZZ _{0/3}	AM _{50/6} ZZ _{0/3}
-112.739eV	-112.754eV	-112.740eV	-112.739eV	-112.739eV	-112.740eV	-112.739eV	-112.752eV

1Ti1Nb -OH

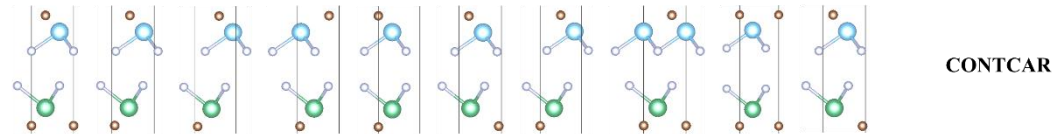
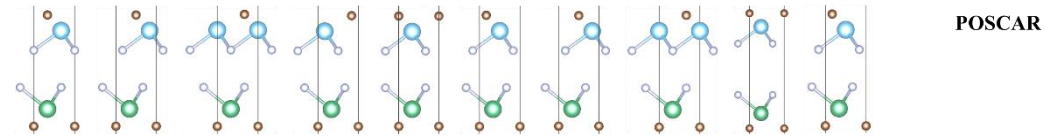


AM ₀ ZZ ₀	AM ₀ ZZ _{6/6}	AM ₀ ZZ _{6/3}	AM ₀ ZZ _{6/2}	AM ₀ ZZ _{26/3}	AM ₀ ZZ _{56/6}	AM _{6/6} ZZ ₀	AM _{6/3} ZZ ₀	AM _{26/3} ZZ ₀	AM _{56/6} ZZ ₀
-125.810eV	-125.811eV	-125.785eV	-125.823eV	-125.786eV	-125.811eV	-125.811eV	-125.823eV	-125.622eV	-125.810eV

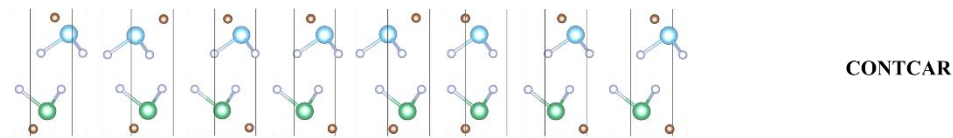
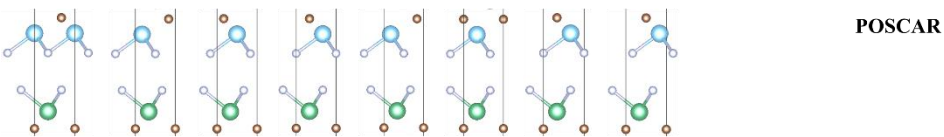


AM _{6/6} ZZ _{6/6}	AM _{6/3} ZZ _{6/6}	AM _{26/3} ZZ _{6/6}	AM _{56/6} ZZ _{6/6}	AM _{6/6} ZZ _{6/3}	AM _{6/3} ZZ _{6/3}	AM _{26/3} ZZ _{6/3}	AM _{56/6} ZZ _{6/3}
-125.784eV	-125.823eV	-125.786eV	-125.784eV	-125.788eV	-125.786eV	-125.784eV	-125.823eV

1Ti3Nb -F

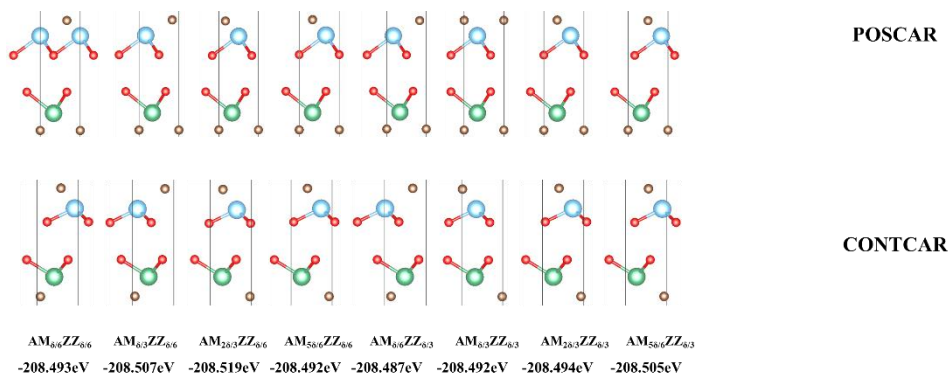
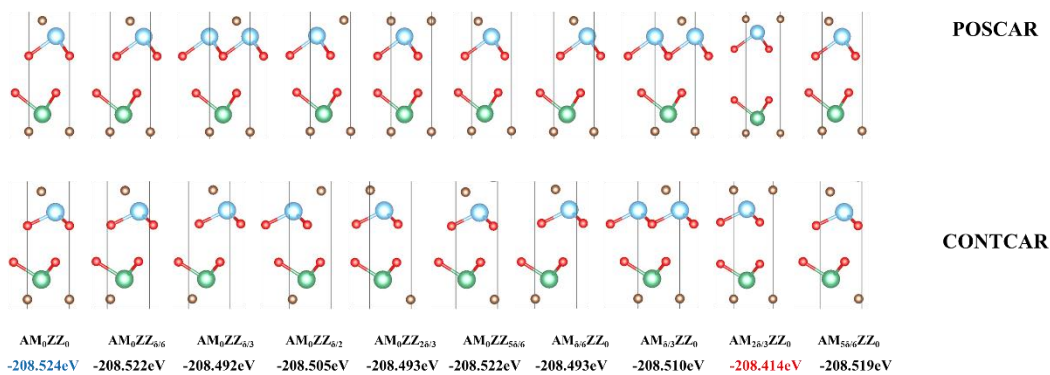


AM ₀ ZZ ₀	AM ₀ ZZ _{6/6}	AM ₀ ZZ _{6/3}	AM ₀ ZZ _{6/2}	AM ₀ ZZ _{26/3}	AM ₀ ZZ _{56/6}	AM _{6/6} ZZ ₀	AM _{6/3} ZZ ₀	AM _{26/3} ZZ ₀	AM _{56/6} ZZ ₀
-185.266eV	-185.266eV	-185.242eV	-185.261eV	-185.242eV	-185.265eV	-185.245eV	-185.265eV	-185.179eV	-185.260eV

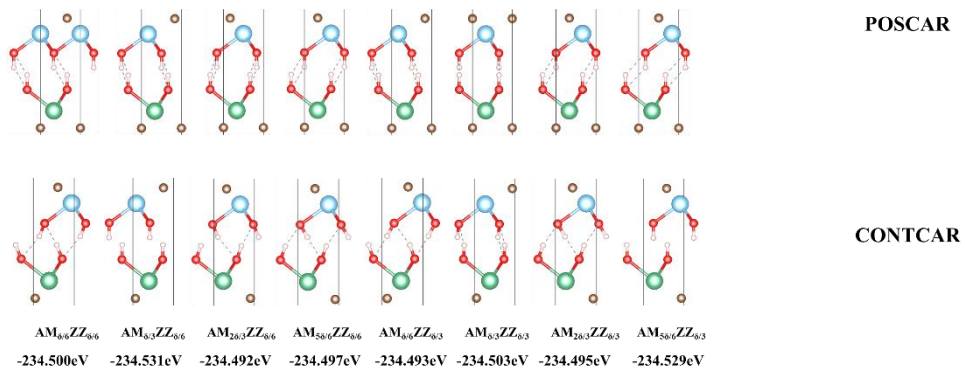
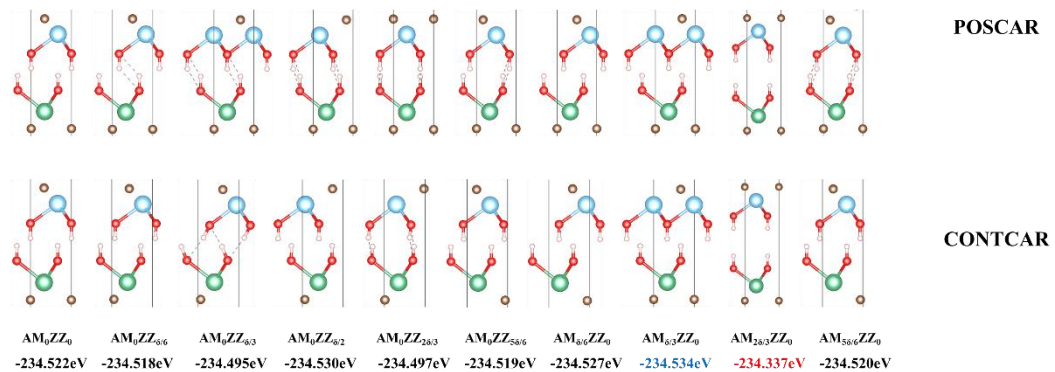


AM _{6/6} ZZ _{6/6}	AM _{6/3} ZZ _{6/6}	AM _{26/3} ZZ _{6/6}	AM _{56/6} ZZ _{6/6}	AM _{6/6} ZZ _{6/3}	AM _{6/3} ZZ _{6/3}	AM _{26/3} ZZ _{6/3}	AM _{56/6} ZZ _{6/3}
-185.244eV	-185.265eV	-185.239eV	-185.243eV	-185.240eV	-185.244eV	-185.243eV	-185.264eV

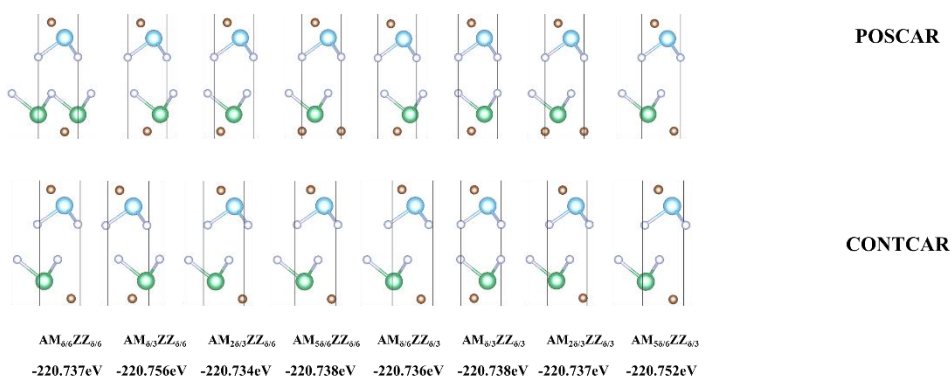
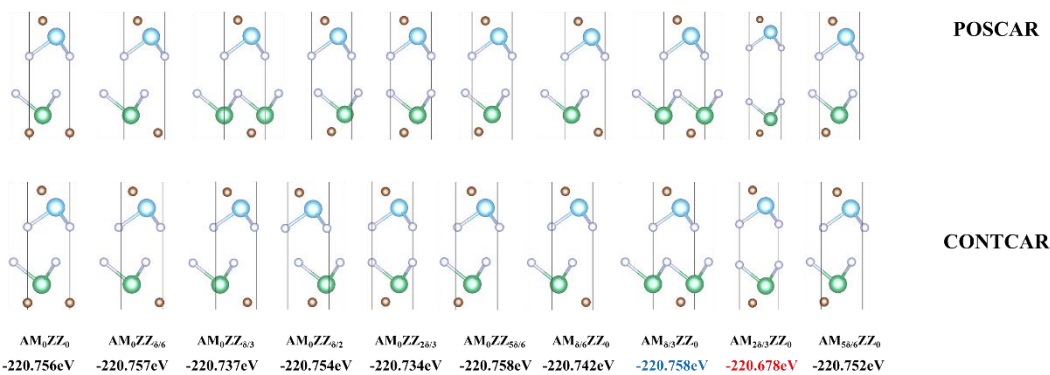
1Ti3Nb -O



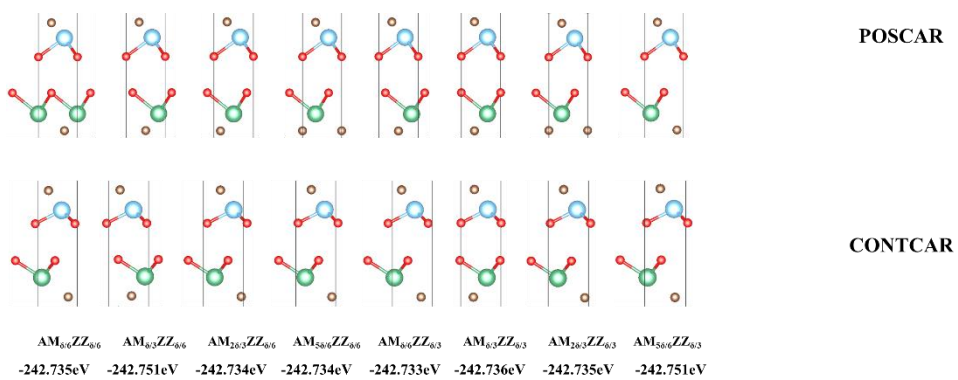
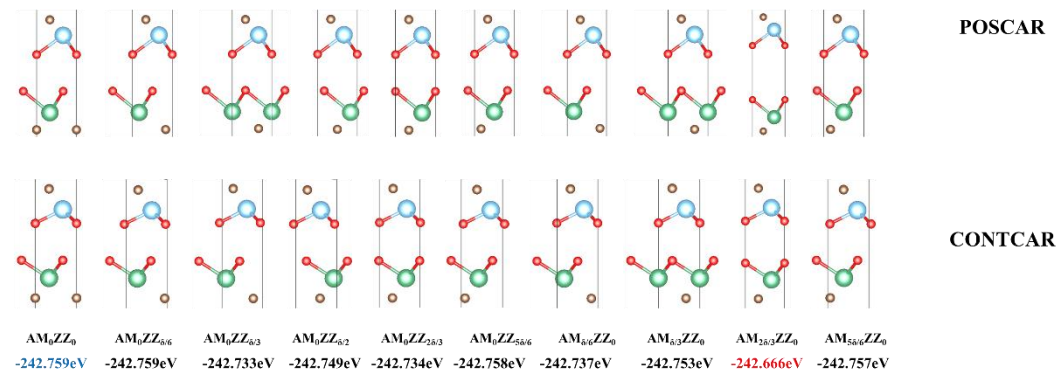
1Ti3Nb -OH



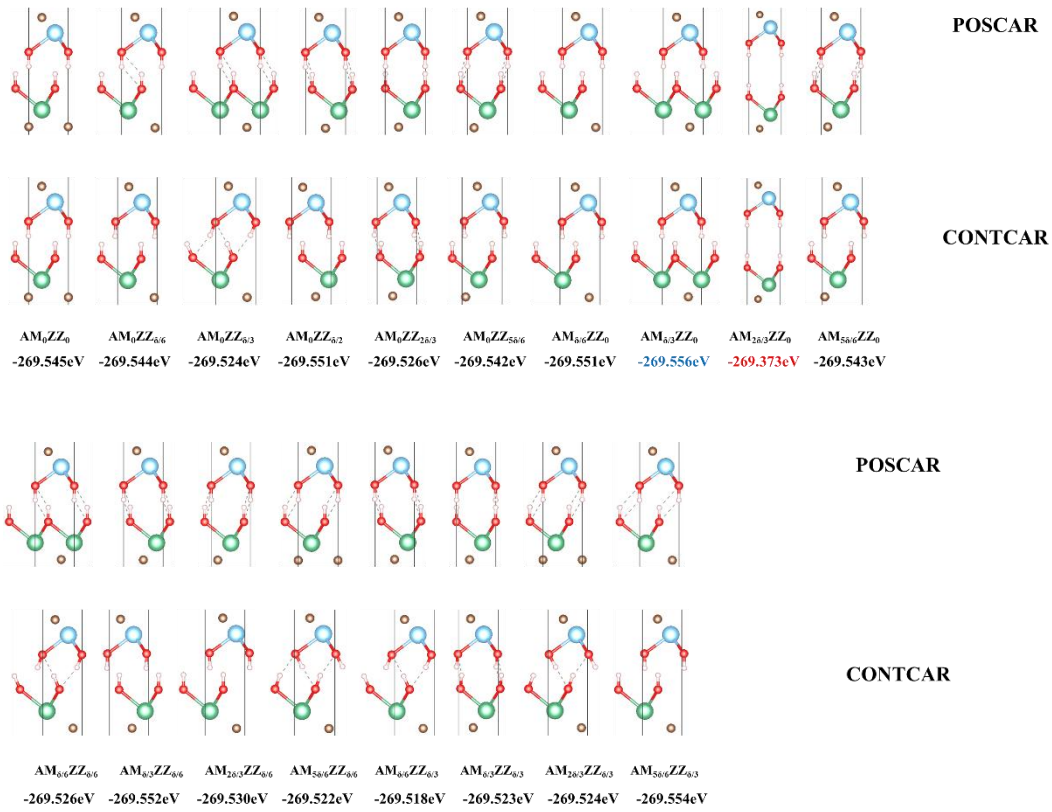
3Ti1Nb -F



3Ti1Nb -O



3Ti1Nb -OH



Appendix II

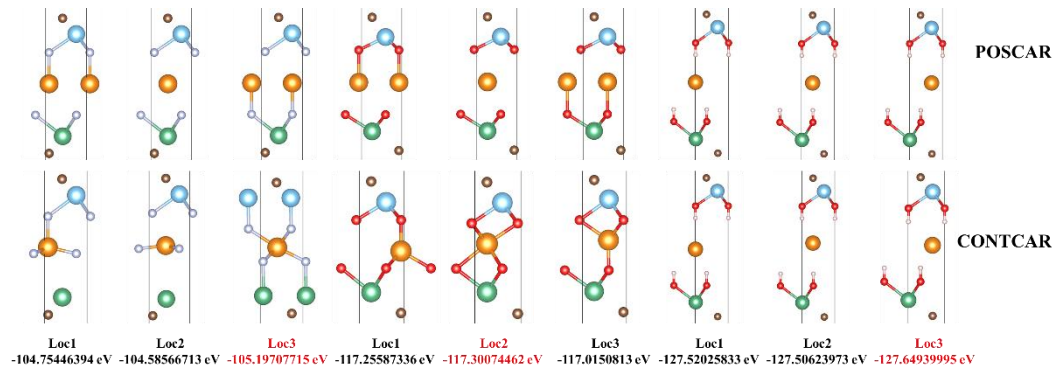
The POSCAR and CONTCAR figures of Ti₃C₂T_x/Nb₂CT_x heterostructures intercalated with Li/Na atoms on the top and bottom, respectively, with systematic listed orderly. The positions and energies of ground states are written in red color. For 2-layer intercalation model, the listed locations refer to the second intercalated atoms. Functional groups are -F, -O and -OH from left to right. For conciseness, only atoms at interspace are displayed.

The legends in appendix I are uniformly provided as follows:

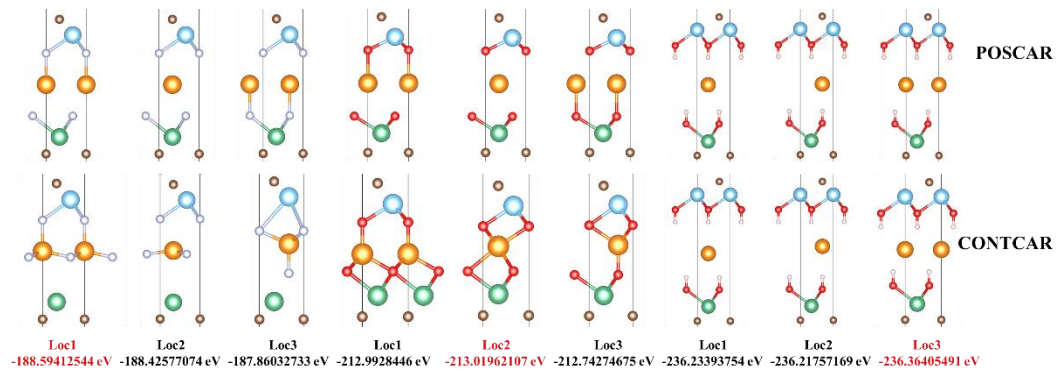


Min Li 1 layer

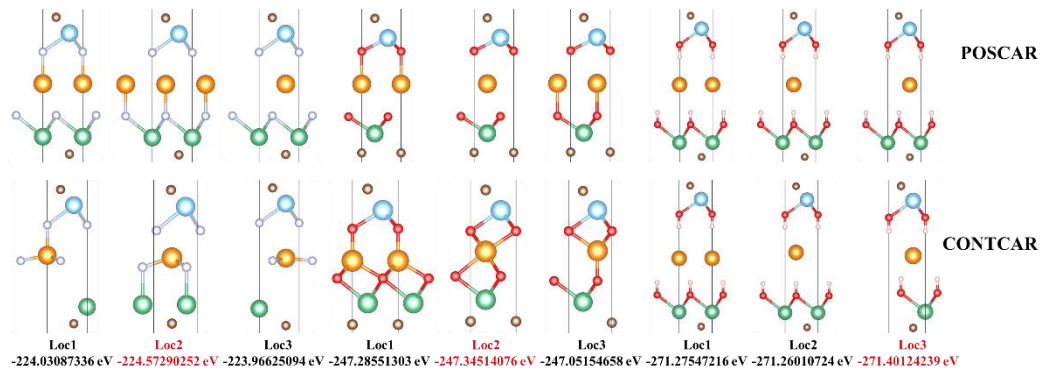
1Ti1Nb



1Ti3Nb

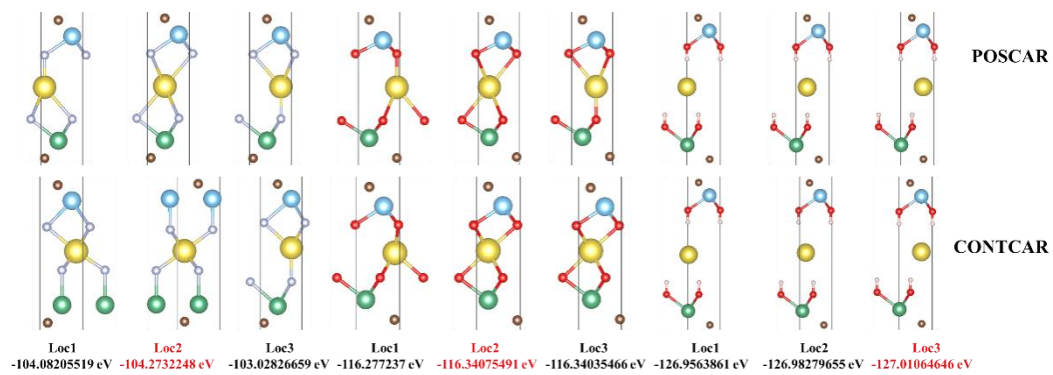


3Ti1Nb

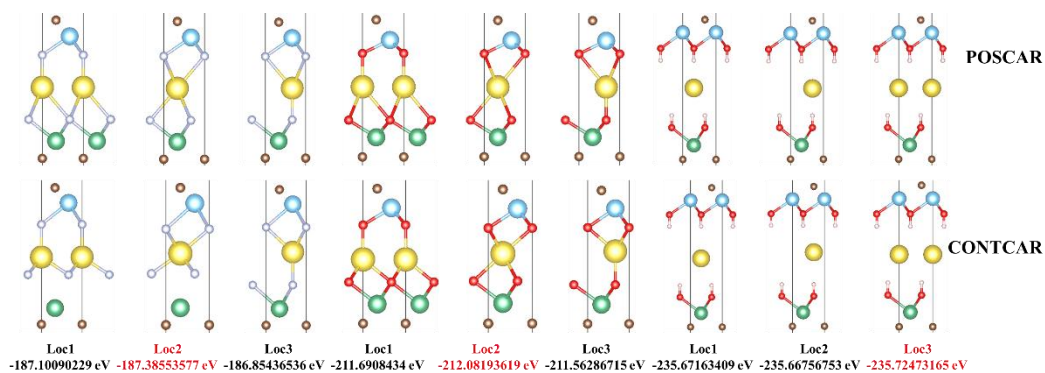


Min Na 1 layer

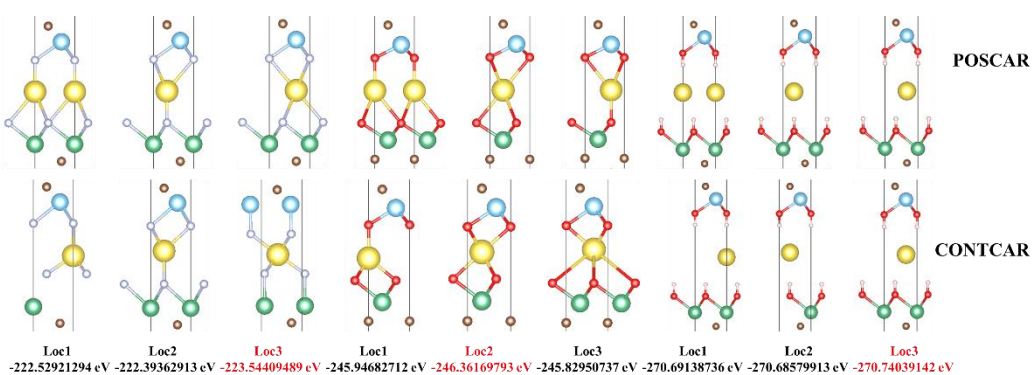
1Ti1Nb



1Ti3Nb

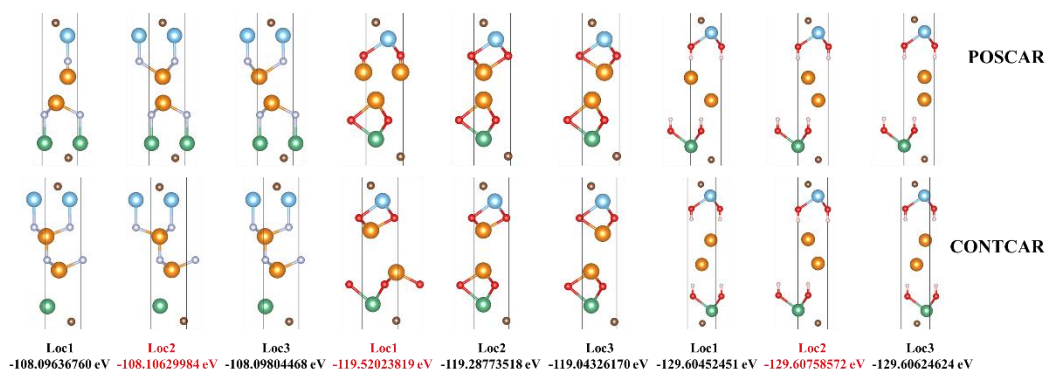


3Ti1Nb

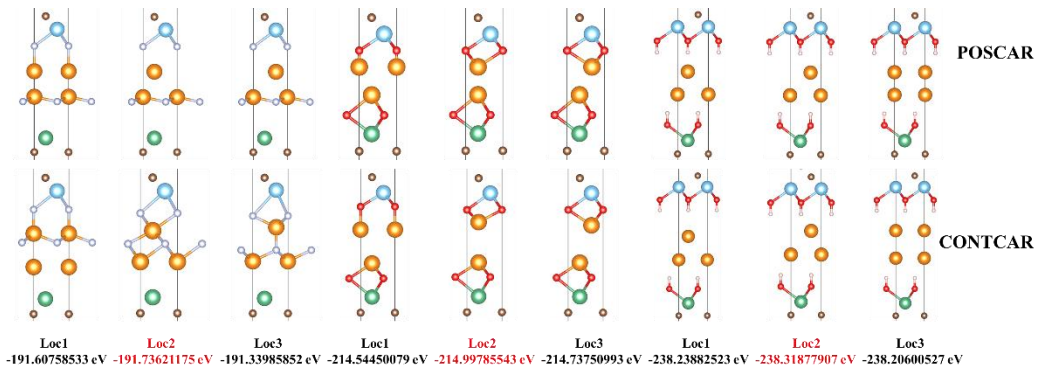


Min Li 2 layer

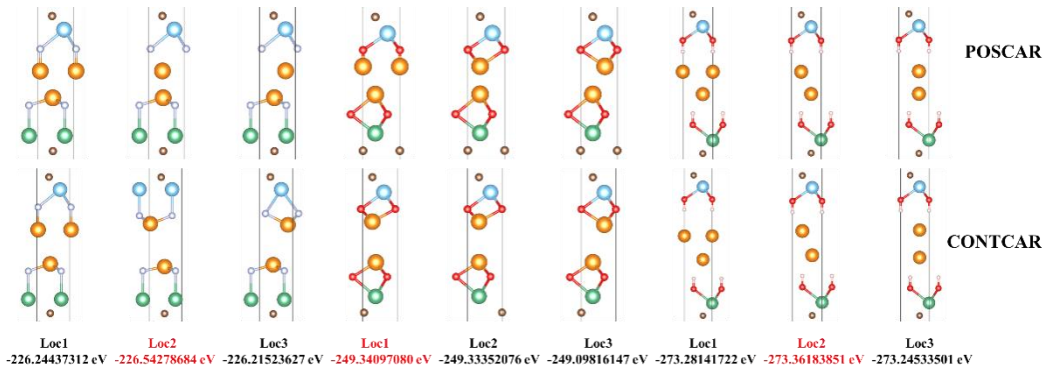
1Ti1Nb



1Ti3Nb

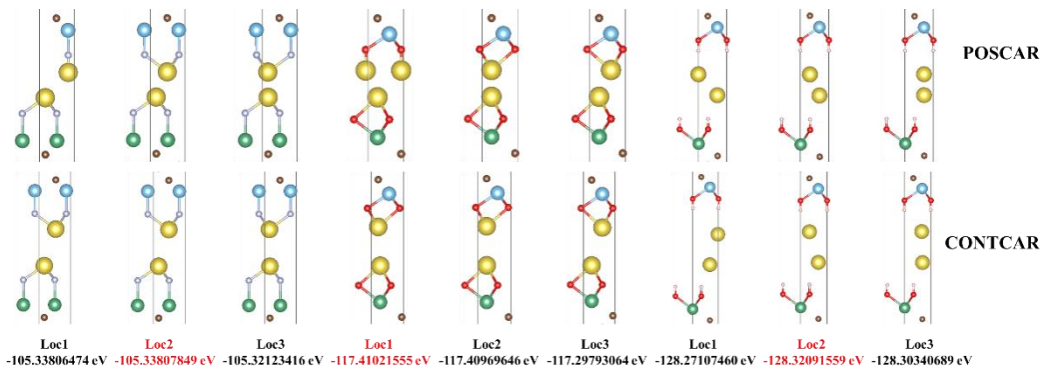


3Ti1Nb

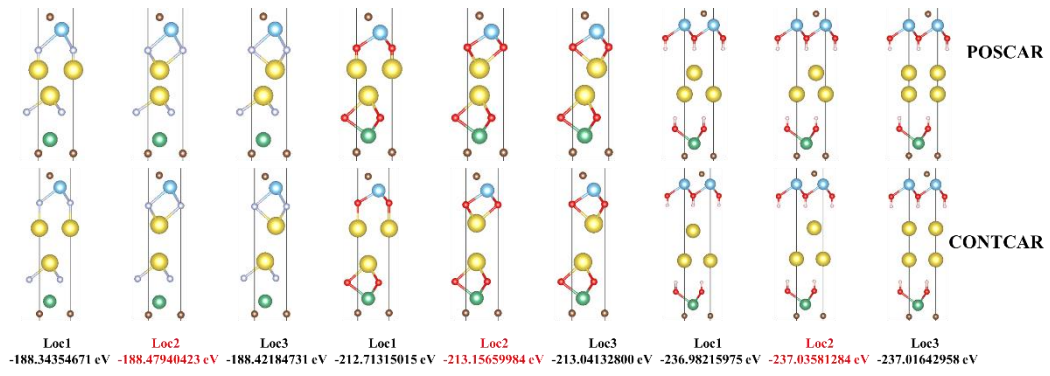


Min Na 2 layer

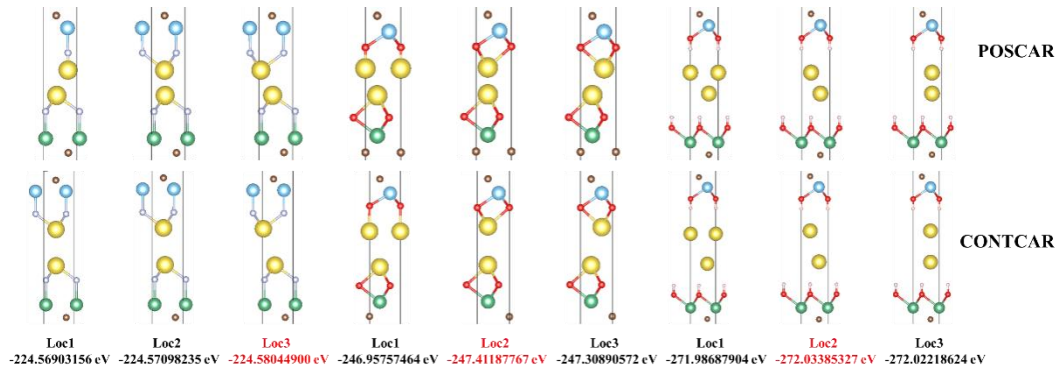
1Ti1Nb



1Ti3Nb

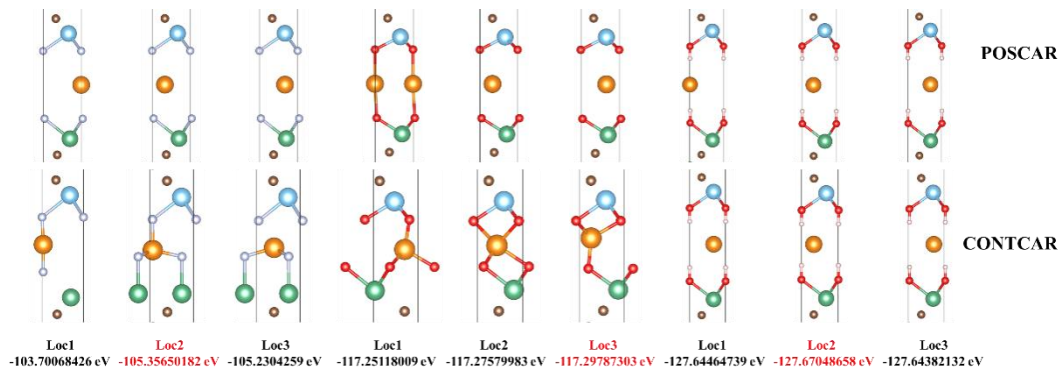


3Ti1Nb

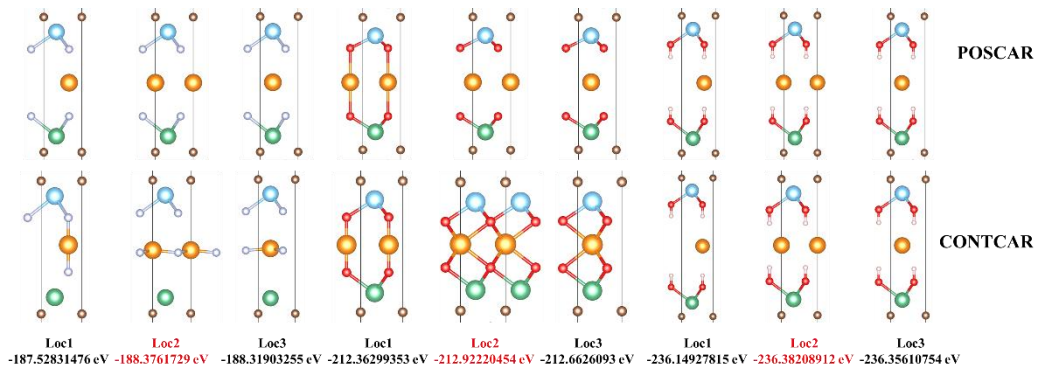


Max Li 1 layer

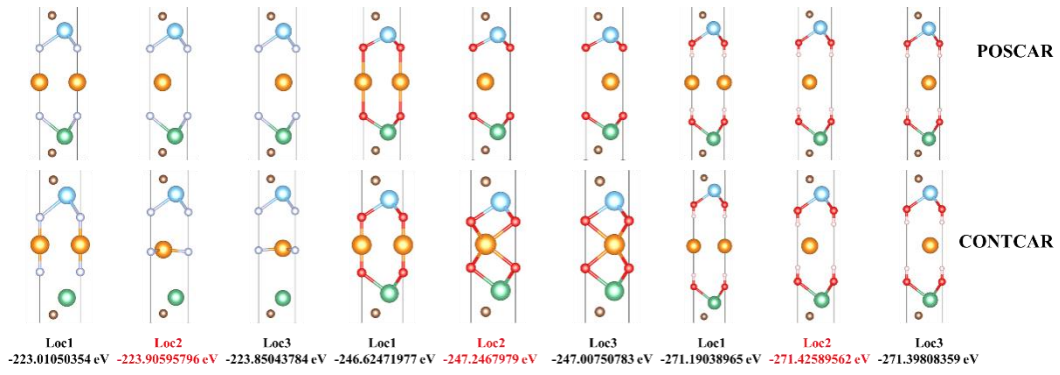
1Ti1Nb



1Ti3Nb

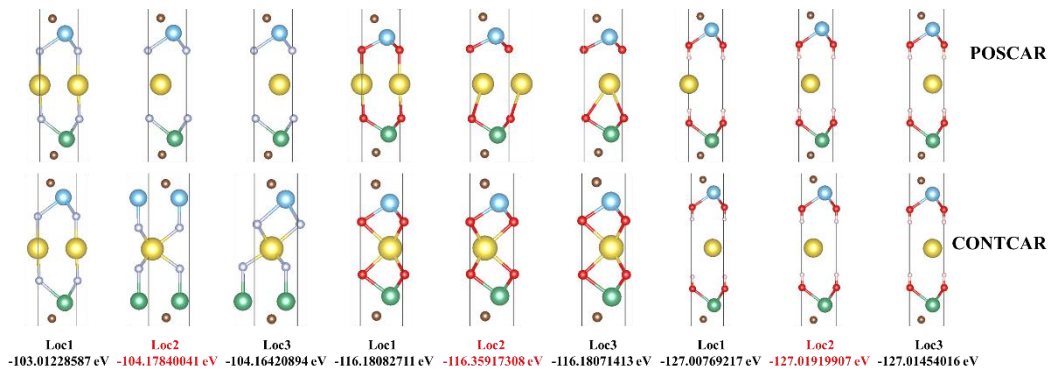


3Ti1Nb

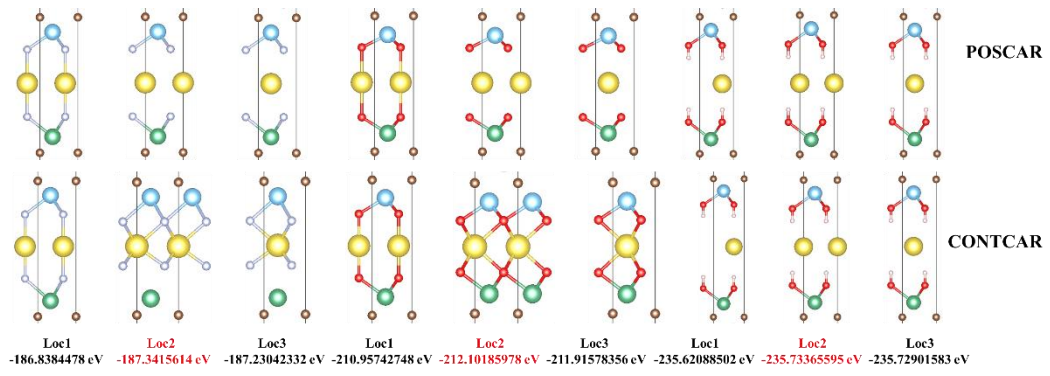


Max Na 1 layer

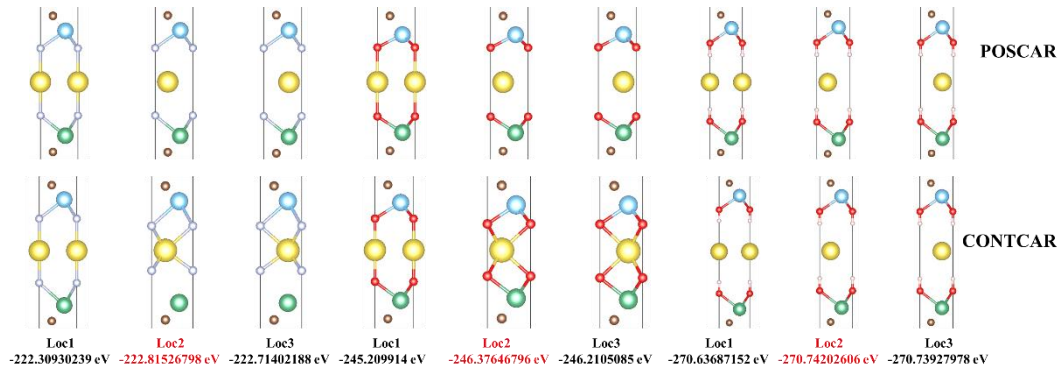
1Ti1Nb



1Ti3Nb

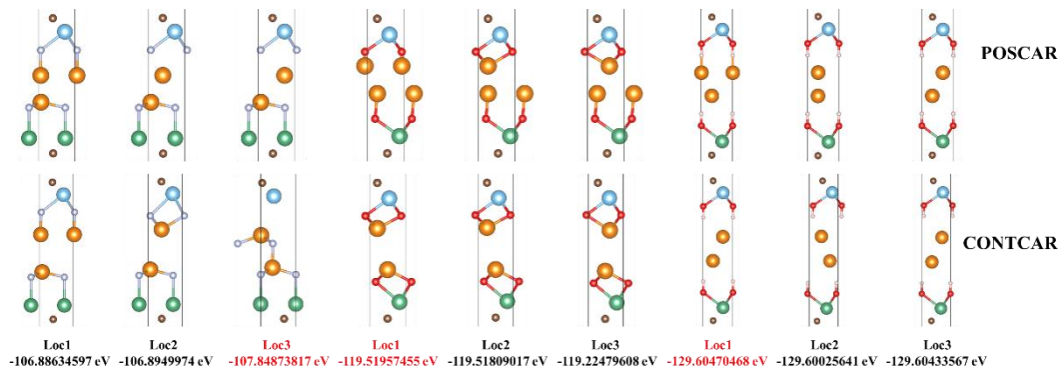


3Ti1Nb

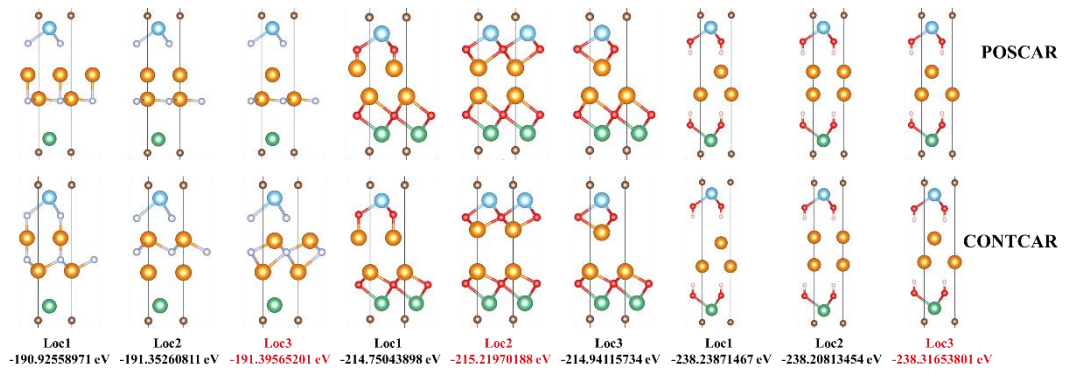


Max Li 2 layer

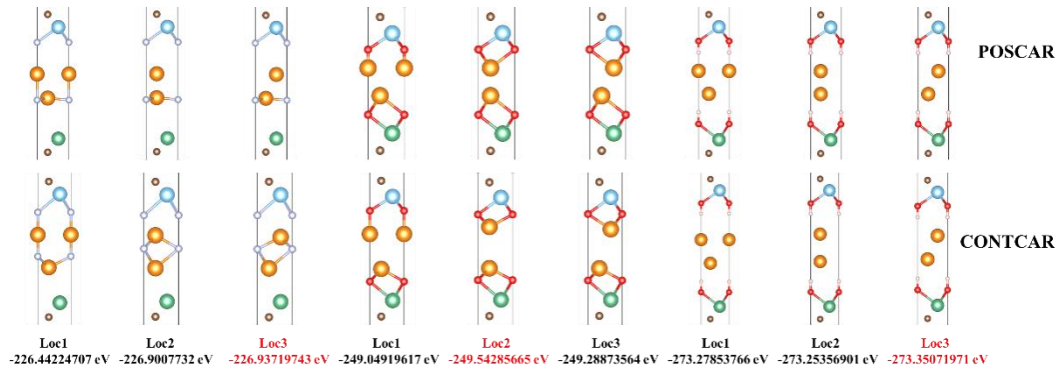
1Ti1Nb



1Ti3Nb

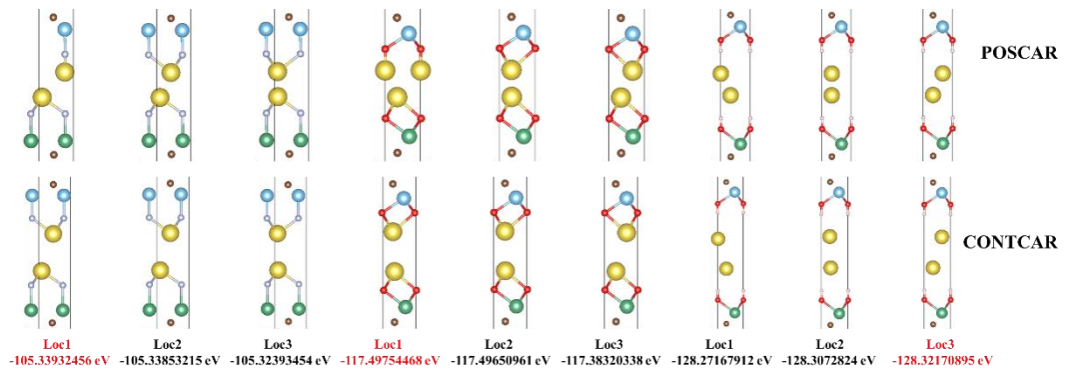


3TiNb

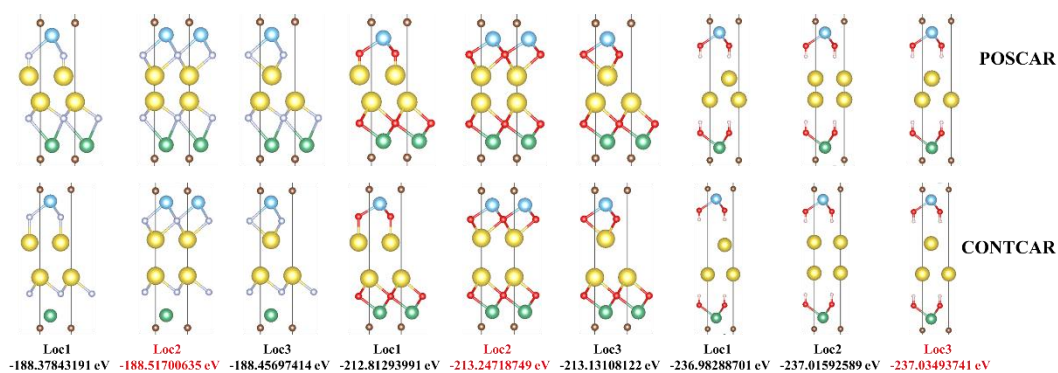


Max Na 2 layer

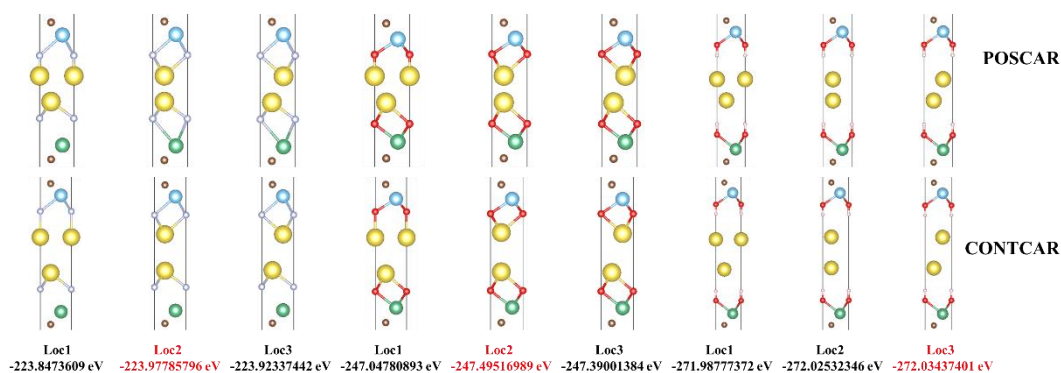
1Ti1Nb



1Ti3Nb



3TiNb



REFERENCES

1. Liu, Y.; Xiao, H.; Goddard, W.A., III. Schottky-Barrier-Free Contacts with Two-Dimensional Semiconductors by Surface-Engineered MXenes. *Journal of the American Chemical Society* **2016**, *138*, 15853-15856, doi:<https://doi.org/10.1021/jacs.6b10834>.
2. Xu, L.; Wu, T.; Kent, P.R.C.; Jiang, D.-e. Interfacial charge transfer and interaction in the MXene/TiO₂ heterostructures. *Physical Review Materials* **2021**, *5*, doi:<https://doi.org/10.1103/PhysRevMaterials.5.054007>.
3. Zhao, S.; Kang, W.; Xue, J. Manipulation of electronic and magnetic properties of M₂C (M = Hf, Nb, Sc, Ta, Ti, V, Zr) monolayer by applying mechanical strains. *Applied Physics Letters* **2014**, *104*, doi:<https://doi.org/10.1063/1.4870515>.
4. Xie, Y.; Dall'Agnesse, Y.; Naguib, M.; Gogotsi, Y.; Barsoum, M.W.; Zhuang, H.L.; Kent, P.R.C. Prediction and Characterization of MXene Nanosheet Anodes for Non-Lithium-Ion Batteries. *Acs Nano* **2014**, *8*, 9606-9615,

doi:<https://doi.org/10.1021/nn503921j>.

5. Aierken, Y.; Sevik, C.; Gulseren, O.; Peeters, F.M.; Cakir, D. MXenes/graphene heterostructures for Li battery applications: a first principles study. *Journal of Materials Chemistry A* **2018**, *6*, 2337-2345, doi:<https://doi.org/10.1039/c7ta09001c>.
6. Kazemi, S.A.; Wang, Y. Super strong 2D titanium carbide MXene-based materials: a theoretical prediction. *J Phys Condens Matter* **2020**, *32*, 11LT01, doi:<https://doi.org/10.1088/1361-648X/ab5bd8>.
7. Fu, Z.H.; Zhang, Q.F.; Legut, D.; Si, C.; Germann, T.C.; Lookman, T.; Du, S.Y.; Francisco, J.S.; Zhang, R.F. Stabilization and strengthening effects of functional groups in two-dimensional titanium carbide. *Physical Review B* **2016**, *94*, doi:<https://doi.org/10.1103/PhysRevB.94.104103>.
8. Hu, T.; Yang, J.; Li, W.; Wang, X.; Li, C.M. Quantifying the rigidity of 2D carbides (MXenes). *Physical Chemistry Chemical Physics* **2020**, *22*, 2115-2121, doi:<https://doi.org/10.1039/c9cp05412j>.
9. Tian, S.; Zhou, K.; Huang, C.-Q.; Qian, C.; Gao, Z.; Liu, Y. Investigation and understanding of the mechanical properties of MXene by high-throughput computations and interpretable machine learning. *Extreme Mechanics Letters* **2022**, *57*, doi:<https://doi.org/10.1016/j.eml.2022.101921>.